The Journal of Wildlife Management 1–21; 2021; DOI: 10.1002/jwmg.21985

Research Article

Habitat Features Predict Carrying Capacity of a Recovering Marine Carnivore

M. TIM TINKER,[1,2] *U.S. Geological Survey, Western Ecological Research Center, Santa Cruz Field Station, 2885 Mission Street, Santa Cruz, CA 95060, USA*

JULIE L. YEE, *U.S. Geological Survey, Western Ecological Research Center, Santa Cruz Field Station, 2885 Mission Street, Santa Cruz, CA 95060, USA*

KRISTIN L. LAIDRE, *Polar Science Center, Applied Physics Laboratory, University of Washington, 1013 NE 40th Street, Seattle, WA 98105, USA*

BRIAN B. HATFIELD, *U.S. Geological Survey, Western Ecological Research Center, Santa Cruz Field Station, 2885 Mission Street, Santa Cruz, CA 95060, USA*

MICHAEL D. HARRIS, *California Department of Fish and Wildlife, Office of Spill Prevention and Response—Veterinary Services, 1385 Main Street, Morro Bay, CA 93442, USA*

JOSEPH A. TOMOLEONI, *U.S. Geological Survey, Western Ecological Research Center, Santa Cruz Field Station, 2885 Mission Street, Santa Cruz, CA 95060, USA*

TOM W. BELL, *Earth Research Institute, University of California, Santa Barbara, Santa Barbara, California, 93106, USA*

EMILY SAARMAN, *Partnership for Interdisciplinary Studies of Coastal Oceans (PISCO), Long Marine Laboratory, 115 McAllister Way, University of California, Santa Cruz, CA 95060, USA*

LILIAN P. CARSWELL, *U.S. Fish and Wildlife Service, Ventura, CA 93003, USA*

A. KEITH MILES, *U.S. Geological Survey, Western Ecological Research Center, 3020 State University Drive, Sacramento, CA 95819, USA*

ABSTRACT The recovery of large carnivore species from over-exploitation can have socioecological effects; thus, reliable estimates of potential abundance and distribution represent a valuable tool for developing management objectives and recovery criteria. For sea otters (*Enhydra lutris*), as with many apex predators, equilibrium abundance is not constant across space but rather varies as a function of local habitat quality and resource dynamics, thereby complicating the extrapolation of carrying capacity (K) from one location to another. To overcome this challenge, we developed a state-space model of density-dependent population dynamics in southern sea otters (*E. l. nereis*), in which K is estimated as a continuously varying function of a suite of physical, biotic, and oceanographic variables, all described at fine spatial scales. We used a theta-logistic process model that included environmental stochasticity and allowed for density-independent mortality associated with shark bites. We used Bayesian methods to fit the model to time series of survey data, augmented by auxiliary data on cause of death in stranded otters. Our model results showed that the expected density at K for a given area can be predicted based on local bathymetry (depth and distance from shore), benthic substrate composition (rocky vs. soft sediments), presence of kelp canopy, net primary productivity, and whether or not the area is inside an estuary. In addition to density-dependent reductions in growth, increased levels of shark-bite mortality over the last decade have also acted to limit population expansion. We used the functional relationships between habitat variables and equilibrium density to project estimated values of K for the entire historical range of southern sea otters in California, USA, accounting for spatial variation in habitat quality. Our results suggest that California could eventually support 17,226 otters (95% CrI = 9,739–30,087). We also used the fitted model to compute candidate values of optimal sustainable population abundance (OSP) for all of California and for regions within California. We employed a simulation-based approach to determine the abundance associated with the maximum net productivity level (MNPL) and propose that the upper quartile of the distribution of MNPL estimates (accounting for parameter uncertainty) represents an appropriate threshold value for OSP. Based on this analysis, we suggest a candidate value for OSP (for all of California) of 10,236, which represents 59.4% of projected K. © 2021 The Authors. *The Journal of Wildlife Management* published by Wiley Periodicals LLC on behalf of The Wildlife Society.

KEY WORDS Bayesian state-space model, density dependence, *Enhydra lutris*, habitat quality, optimal sustainable population, population abundance, sea otter.

Received: 22 April 2020; Accepted: 17 November 2020

This is an open access article under the terms of the Creative Commons Attribution-NonCommercial-NoDerivs License, which permits use and distribution in any medium, provided the original work is properly cited, the use is non-commercial and no modifications or adaptations are made.

[1]*E-mail: ttinker@ucsc.edu*

[2]*Current affiliation: Ecology and Evolutionary Biology, UC Santa Cruz, Long Marine Lab, 115 McAllister Way, Santa Cruz, CA 95060, USA*

After decades of legal protection and conservation efforts, some of the world's most depleted and endangered wildlife populations are recovering and re-colonizing regions from which they had once been extirpated (Halley and Rosell 2002, Heide-Jørgensen et al. 2007, Ripple and Beschta 2007, Buxton et al. 2014, Silliman et al. 2018). Although encouraging, this recovery process is sometimes associated with new conservation and management challenges. Particularly in the case of large predators, their return to ecosystems from where they were missing for long periods may cause substantial perturbations to local food web dynamics (Ripple and Beschta 2012). Returning large predators to ecosystems can lead to direct human-wildlife conflict or to resource-use conflicts with human economies that developed during their absence (Carswell et al. 2015). At the same time, the recovery of large predators can help restore ecosystem functioning, sometimes in unanticipated ways, and fuel the growth of new economic opportunities (Lotze et al. 2006, Beschta and Ripple 2009). Anticipating the ecological and socioeconomic effects of large predator recovery requires first answering a suite of questions that can be summarized as when, where, and how many? The question of when relates to the speed of recovery, which requires information on growth rates and dynamics of population expansion into un-occupied suitable areas. The question of where refers to the specifics of location and distribution (current and future) within a species' potential range, which requires information on habitat associations or environmental predictors of occupancy and abundance. The question of how many refers to the expected future abundance of the species once it has fully recovered; this requires information on environmental carrying capacity (K), or the number of animals that can be supported in a given area once the population has reached equilibrium with its limiting resources. Estimating K is complicated because equilibrium abundance can vary as a function of prey productivity and habitat quality (Hobbs and Swift 1985) and thus cannot be simply extrapolated from one location to others. A further complication is that changing environmental conditions (e.g., anthropogenic influences, climate change effects) can lead to variation in K over time.

Sea otters (*Enhydra lutris*) provide an excellent example of a recovering coastal marine predator whose return to regions from which it was extirpated during the fur trade of the eighteenth and nineteenth century (Kenyon 1969) can have substantial ecological and (in some cases) socioeconomic effects (Larson et al. 2013, Salomon et al. 2015). As a keystone carnivore in nearshore marine ecosystems, sea otters have a disproportionately large influence on the structure and function of subtidal food webs (Estes and Palmisano 1974). Many of the changes associated with the return of sea otters to these systems are considered beneficial; these include an increase in growth and productivity of dominant primary producers such as kelp and eelgrass (*Zostera* spp.; Estes and Duggins 1995, Hughes et al. 2013), greater diversity and productivity of invertebrate assemblages (Duggins 1980, Estes et al. 2004), and improved nursery habitat for commercially important fish (Reisewitz et al. 2006). But in some areas, the return of sea otters can lead to conflicts with commercial, recreational, and subsistence fisheries that were made possible by the super-abundance of certain invertebrate taxa that occurred when sea otters were removed from the system (Carswell et al. 2015). Resource managers thus face the dual challenge of ensuring full recovery of depleted sea otter populations, while anticipating and addressing potential socioeconomic changes that are likely to occur. Successful resolution of conflicts between fisheries and recovering marine bird and mammal populations depends on early engagement with stakeholders and availability of reliable scientific data on spatially explicit dynamics and population potential (Bruckmeier et al. 2013, Jepsen and Olesen 2013, Klenke et al. 2013, Butler et al. 2015, McDonald et al. 2016).

The southern sea otter (*E. l. nereis*) is listed as threatened under the United States Endangered Species Act (ESA) and is also protected under the United States Marine Mammal Protection Act (MMPA). The MMPA established federal policy that marine mammal species and stocks should not be allowed to diminish below their optimum sustainable population (OSP), defined as the number of animals resulting in maximum productivity, keeping in mind the carrying capacity of the habitat and the health of the ecosystem of which they are a part (16 United States Code [USC] 1362). Species or stocks that are listed under the ESA are automatically considered to be depleted under the MMPA, but designation of depleted status for non-ESA-listed species may also result from a determination that a species or stock is below its OSP (16 USC 1362). Because an estimate of carrying capacity (K) forms the basis for determination of a species or stock's OSP and hence its depleted status, estimating K for each designated stock of sea otters is a high priority for management under the MMPA.

The southern sea otter's current distribution in central California, USA, ranging from approximately Pigeon Point in the north to Gaviota State Park (20 km east of Point Conception) in the south (Fig. 1), represents just a fraction of its historical distribution, which includes all the coastal waters of California and portions of coastal Oregon, USA, and Baja, Mexico (U.S. Fish and Wildlife Service [USFWS] 2003). Anticipating the potential equilibrium abundance of sea otters in currently occupied areas and in uncolonized but potential future habitats is a high priority for managers. A first step in achieving this goal is to define the spatial scale at which K is to be measured or estimated. There is growing recognition that sea otter populations are structured at fairly small spatial scales (Bodkin 2015, Davis et al. 2019, Tinker et al. 2019*a*) because of the limited mobility and high site fidelity of reproductive females (Tarjan and Tinker 2016, Breed et al. 2017) and because the abundance of their benthic invertebrate prey varies at small spatial scales and is subject to local depletion (Burt et al. 2018). Demographically, K for sea otters is determined at local scales (i.e., over tens of kilometers rather than over hundreds of kilometers), and a regional value of K is better understood as the summation of K over all local habitats. This recognition shifts the challenge to understanding how local K varies over space (and potentially over time), and what explains this variation.

The equilibrium density for any species depends on the dynamics of ≥1 limiting resources. For many upper-trophic-level predators (sea otters included), the key limiting resource

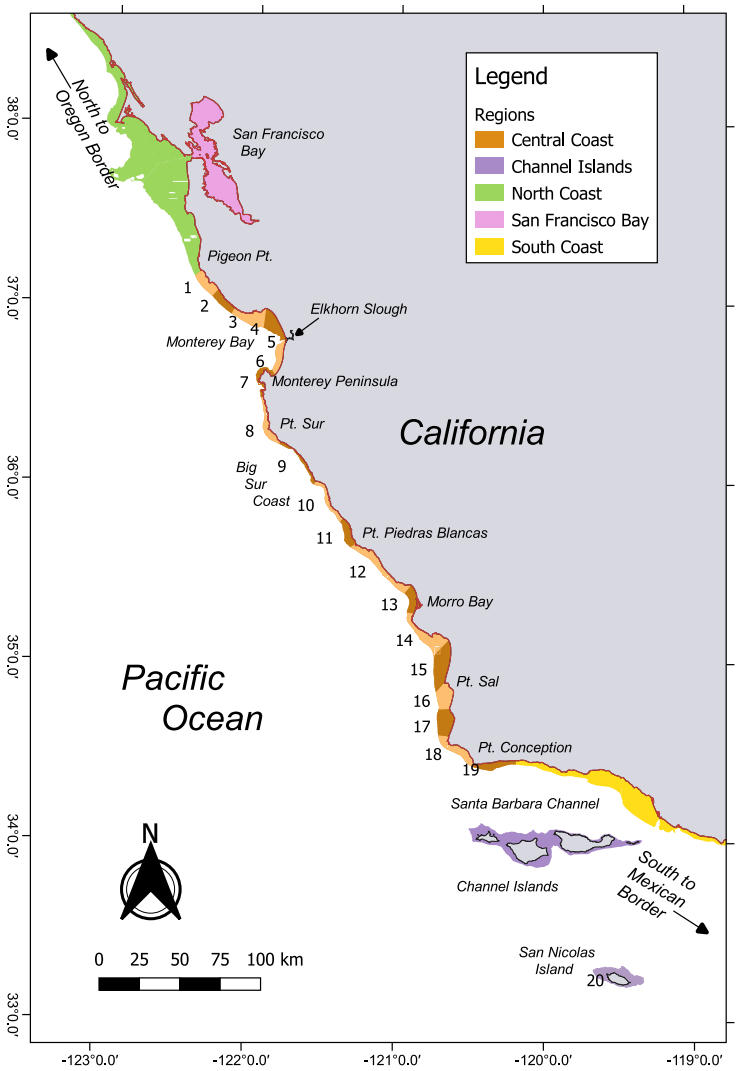

Figure 1. The central coast of California, USA, showing the main study area. Sea otter habitat (both currently occupied and potential) is shown as a colored band along the coast, color-coded to identified 5 main regions used to summarize model projections. The central coast region is further sub-divided into 19 coastal sections (labeled with numbers), with a twentieth section around San Nicolas Island in the Channel Islands; we used these 20 coastal sections to analyze population trends between 1983 and 2018, and they represent the currently occupied (as of 2018) areas of the coast.

is high-quality prey (Estes 1979, Estes et al. 1996). Therefore, spatial variation in the abundance and productivity of benthic macro-invertebrates is the factor most likely to predict local variation in *K* for sea otters. Unfortunately, many sea otter prey are highly cryptic and their abundance is logistically difficult to quantify at relevant scales. Luckily there are a number of possible habitat-based proxies for invertebrate prey productivity, and several previous analyses have used habitat-based predictors of sea otter abundance or carrying capacity (Laidre et al. 2001, Coletti 2006, Gregr et al. 2008, Laidre et al. 2009, Stewart et al. 2015). Laidre et al. (2001) analyzed the relationship between sea otter density and benthic substrate, then extrapolated an estimate of *K* for all of California. This estimate of *K* has served as a useful benchmark for coastal resource managers for almost 2 decades; however, a re-analysis of *K* for southern sea otters is warranted for several reasons. The single habitat predictor used for the earlier analysis was a relatively simple classification of substrate type (rocky, sandy, mixed), but researchers have reported that sea otter abundance and foraging success are affected by a broader array of environmental features including coastal bathymetry (Thometz et al. 2016), kelp canopy cover (Nicholson et al. 2018), benthic substrate complexity and composition (Stewart et al. 2015, Tinker et al. 2017), and ocean productivity (Davis et al. 2019). We now understand that estuarine systems may represent important sea otter habitat, distinct from soft-sediment areas of the outer coast (Hughes et al. 2013, Silliman et al. 2018). Recent innovations in remote sensing, substrate characterization using multi-beam sonar, and analysis using geographic information systems (GIS) have made data available for all these habitat features in coastal California waters, thereby enabling a more comprehensive examination of habitat predictors of carrying capacity.

A second limitation of the analysis by Laidre et al (2001) was the assumption that certain areas of the coast had

reached carrying capacity by the late 1990s; they used these index areas as the basis for extrapolating substrate-specific values for equilibrium density. It is now recognized that the apparent leveling off of sea otter abundance in California between 1995 and 2000 was a brief period of population decline caused by elevated mortality in the geographic center of their range (Tinker et al. 2006), and positive growth resumed in the early 2000s (Tinker and Hatfield 2017). Thus, some of the index areas used by Laidre et al (2001) were likely still below *K*, and the estimated equilibrium density values therefore were biased to some degree. Recently developed analytical methods offer a more robust approach for estimating *K*, circumventing the need to assume equilibrium status of any one index area. Specifically, by fitting Bayesian state-space models to time series of survey data, it is possible to estimate the parameters of a theta-logistic growth model, including *K* (Miller and Meyer 2000, Chaloupka and Balazs 2007, Wang 2007). Similar methods have been used recently to estimate local and regional values of *K* for sea otters in southeast Alaska (Tinker et al. 2019*a*).

We developed a method for estimating the functional relationship between habitat features and carrying capacity for the southern sea otter. We used a state-space model of density-dependent population dynamics, in which *K* is estimated as a continuously varying function of a suite of physical, biotic, and oceanographic variables, all described at fine spatial scales. We fit the model to a time series of spatially explicit survey data, incorporating auxiliary data on non-density-dependent mortality sources to improve model fit and generalizability. We used the results to project estimated values of *K* to the entire historical range of southern sea otters in California. We designed our analyses to determine whether habitat-based predictor variables can identify key areas of the coast capable of supporting high density sea otter populations, the expected equilibrium abundance of sea otters across their entire range in California, and an appropriate candidate value for OSP in California.

STUDY AREA

Our analyses apply to all potential sea otter habitat (9,580 km^2; Fig. 1) in coastal California, over the period 1983–2018. Sea otter habitat has been defined previously as all coastal marine intertidal and subtidal areas between the shoreline and the 100-m depth contour (Bodkin et al. 2004), although other studies have limited consideration to the 0–40-m depth range (Gregr et al. 2008). Based on preliminary analysis of survey data (Tinker and Hatfield 2017) and published information on diving depths of sea otters in California (Tinker et al. 2007, Thometz et al. 2016), we defined potential sea otter habitat in California as the marine coastal zone between 0–60 m in depth, including tidally influenced estuaries. This region is part of the California Current and is characterized by cool, nutrient-rich waters and strong seasonal upwelling caused by prevailing northwesterly winds between May and September (Lynn and Simpson 1987). Seasonal fluctuations in temperatures and rainfall are typical of temperate, Mediterranean-like climates, with a long summer dry season (May–Nov) and slightly cooler and wetter winters (Dec–Apr).

The intertidal and nearshore subtidal zones in coastal California include a mix of complex rocky areas interspersed with soft-sediment areas, the latter including several large, sand-bottomed embayments. In rocky reef areas, macroalgae (i.e., kelp) forms the dominant vegetation, including surface canopy-forming kelp species (giant kelp [*Macrocystis pyrifera*] and bull kelp [*Nereocystis luetkeana*]) and various understory kelps (including brown and red algae species), which together comprise a kelp forest (Schiel and Foster 2015). Diverse assemblages of macro-invertebrates and fish species rely on these kelp forests for food and physical habitat structure (Miller et al. 2018). Larger vertebrate predators (seals, seabirds, sea otters) represent the upper trophic levels of these kelp-associated food webs, with sea otter diets including virtually all available macro-invertebrate taxa (Riedman and Estes 1990). Sub-tidal food webs in soft-sediment coastal areas differ from kelp forests: phytoplankton represent the predominant primary producers and burrowing infaunal (e.g., clams, marine worms) and epifaunal invertebrates (e.g., crabs, sand dollars) represent the primary prey species for sea otters (Kvitek and Oliver 1988). In addition to the rocky and soft-sediment benthic areas of the outer coast, California features several estuarine ecosystems, defined as semi-enclosed, tidally influenced embayments with freshwater inputs, which experience a mixture of fresh and saline waters and provide important habitat for a variety of marine and terrestrial species (Day et al. 1989). Dominant vegetation includes seagrass (*Zostera marina*) and green algae in sub-tidal areas and pickleweed (*Salicornia virginica*) in the inter-tidal zone. Infaunal invertebrate species (e.g., clams, marine worms) and epifaunal species (e.g., crabs, fish, sharks, rays; Hechinger et al. 2011) can occur at high densities. Sea otters can use any estuarine waters having sufficient tidal exchange to support marine invertebrate prey assemblages; recent evidence suggests that estuarine systems may potentially support higher densities of sea otters than comparable soft-sediment areas along the outer coast (Silliman et al. 2018).

Analyses of sea otter population dynamics and genetics (Gagne et al. 2018, Tinker et al. 2019*a*) indicate that populations are structured and regulated at relatively small spatial scales, tens of kilometers rather than hundreds of kilometers. To accommodate this demographic structure in our analyses, we partitioned all potential sea otter habitat into a contiguous series of coastal sections ($s = 1, 2 \ldots S$), each spanning approximately 20–40 km of coast (Fig. 1). The size of each section was several times larger than a typical sea otter home range (Tarjan and Tinker 2016) and thus demographic processes within a section can be considered homogenous, whereas sea otters in different sections might experience different conditions and limiting factors. We selected boundaries between coastal sections to match the divisions used previously for analyzing sea otter survey

data (Laidre et al. 2001, Tinker et al. 2008); these boundaries correspond to natural breaks between areas of mostly homogenous benthic zone characteristics (Tinker and Hatfield 2017).

METHODS

Data Collection and Processing

Survey data.—We use previously published data from standardized range-wide censuses conducted annually along the central California coast (Hatfield et al. 2018*a*), detailed methods for which are described elsewhere (Tinker and Hatfield 2017). Hatfield et al. (2018*b*) used similar methods to survey the mainland coast and the distinct sea otter population at San Nicolas Island, California. Shore-based survey methods consisted of teams of observers that scanned the entire nearshore central coastal zone using binoculars and high-powered spotting scopes. They marked the location of each individual or group of otters on high-resolution coastal maps (scale 1:24,000) and later digitized locations into a GIS. In areas of the mainland with limited coastal access, or shallow, sandy embayments where sea otters can occur far from shore and thus are difficult to count reliably by shore-based observers, teams used aerial survey methods. They flew aerial surveys along contiguous transects oriented parallel to the shore covering all areas between the coastline and the 60-m depth contour; 2 observers and a data recorder digitized the locations of all observed animals directly into a GIS. We combined data from shore-based and aerial surveys prior to analyses. The resulting data set provides an un-corrected count of the entire population. Because of the un-replicated nature of each year's count, no formal correction is available for the number of un-observed animals for any given survey, a value that likely varies considerably from year to year (Tinker and Hatfield 2017). Also, aerial surveys (which account for ~30% of the mainland count) have a lower and more variable detection probability than shore-based counts, which can detect 90–95% of animals present (Estes and Jameson 1988, Udevitz et al. 1995, Bodkin and Udevitz 1999). A previous investigation of the detection probability of southern sea otters from an aerial platform (which used decoy sea otter targets in replicated trials) suggested a detection probability ranging from 40–80%, depending on viewing conditions (Henkel et al. 2014). Observers did not record viewing conditions for aerial surveys consistently over the study period; thus, selection of an appropriate correction factor for this study was not feasible. Moreover, all management benchmarks for southern sea otters (e.g., criteria for up-listing or down-listing recovery status under the ESA) correspond to an abundance index based on un-corrected counts (USFWS 2003). Given these limitations, and for consistency with management benchmarks and previous publications (Tinker et al. 2006), we did not attempt to correct counts for detection probability or availability, as has been done for northern populations (Bodkin and Udevitz 1999), but instead relied on un-corrected counts that are assumed to capture a high proportion of the population on average (Estes and Jameson 1988). Observers conducted all sea otter surveys with approval and oversight by the Institutional Animal Care and Use Committee of the University of California Santa, Santa Cruz, and with permission of the USFWS Department of Management Authority (permit number MA672624).

We analyzed annual spring count data from mainland coast censuses conducted during 1983–2018 (Hatfield et al. 2018*a*) but excluding 2011 when adverse weather conditions prevented completion of the survey. For San Nicolas Island we used annual spring count data from 1995–2018 (Hatfield et al. 2018*a*). For both time series, raw data consisted of spatially explicit observations of independent otters and dependent pups in groups ≥1. To fit the state-space model, we compiled the raw data into 2 separate and effectively independent data sets. First, we tallied the annual counts in each of the 20 distinct coastal sections (Fig. 1) to obtain the count of independent otters for coastal section s in year t ($C_{s,t}$). Second, we created a high-resolution spatial summary of sea otter distribution by tallying across all years the number of otter observations at each cell of a 100-m grid. We created this 100-m square grid in NAD83 Teale Albers projection (https://spatialreference.org/ref/sr-org/california-teale-albers-nad83-projection, accessed 1 Sep 2019) for the entire coastline of California between the low tide and the 60-m depth contour (see Fig. S1, available online in Supporting Information) and used the grid for summarizing all habitat features (described below). We spatially joined the raw survey data for the mainland and San Nicolas Island to this grid (i.e., assigned each observed otter group the unique identifier of the closest grid cell [g] based on the Euclidean distances between observations and grid centroids) to compute a vector of otter counts summed across survey years for each grid cell (O_g).

Carcass data.—Shark-bite mortality has recently emerged as a major source of mortality for sea otters in California (Tinker et al. 2016, Moxley et al. 2019, Miller et al. 2020). Variation in *per capita* risk of shark bite may be explained in part by proximity to pinniped haul-out areas and availability of kelp canopy cover (Tinker et al. 2016, Nicholson et al. 2018) but appears to be largely independent of sea otter population density (Miller et al. 2020). To the extent that elevated rates of shark-bite mortality are influencing local population trends (Hatfield et al. 2018*b*) and are functionally density-independent, they could complicate the detection of density-dependent trends. Therefore, to avoid confounding effects and improve fit of the state-space model, we tracked this source of mortality separately from all other sources of mortality that are largely density-dependent. To improve fit, we used a previously published data set documenting all sea otter strandings in California from 1985–2017 (Hatfield et al. 2017). Moribund and dead sea otters frequently wash ashore in California, where they may be found and reported by the general public and are then collected by members of a coordinated state-wide sea otter stranding response network. The objective of the network is to document and recover all stranded southern

sea otters, although certain areas such as the Big Sur coastline are under-represented because of access and logistical constraints. Members examine all beach-cast sea otters (most of which are dead, but also live moribund animals that would have died without intervention) and record the date, geographic location, sex, age class, general condition, and circumstantial cause(s) of death (if evidence is apparent) of each recovered animal. Shark-bite wounds in particular leave very clear evidence (puncture wounds), and with the exception of heavily decomposed or scavenged carcasses, cause of death from sharks can be reliably distinguished from all other causes of death (Tinker et al. 2016, Hatfield et al. 2017). For each year and coastal section, we tabulated the number of recovered carcasses ($Z_{s,t}$) and the number of carcasses with shark bite as likely cause of death ($Z_{sb,s,t}$). We tallied data separately for males and females and excluded from analyses a small number of decomposed or scavenged carcasses where determination of shark-bite status (or any other cause of death) could not be reliably determined.

Habitat variables.—Physical variables that affect sea otter density include bathymetric depth and substrate type (Laidre et al. 2001, 2009; Bodkin et al. 2004; Tinker et al. 2017, 2019*a*). In California, we collected bathymetric data describing depths (in m) from the coastline out to 20 km from shore using high-resolution multibeam mapping by the California Seafloor mapping program (Johnson et al. 2017), although we used some legacy data to fill in gaps in coverage, especially in southern California (California Department of Fish and Wildlife, Marine Region GIS downloads, ftp://ftp.dfg.ca.gov/R7_MR/BATHYMETRY, accessed 1 Sep 2019). Next, we classified multibeam bathymetry data into 2 categories of benthic substrate, corresponding approximately to rocky versus soft sediment, using the vector ruggedness measure (VRM) tool in ArcGIS (version 10.4+; Esri, Redlands, CA, USA), part of the Benthic Terrain Modeler toolbox (https://coast.noaa.gov/digitalcoast/tools/btm.html, accessed 1 Sep 2019) provided by the National Oceanic and Atmospheric Administration's Office for Coastal Management. We completed most substrate classifications based on the California Seafloor mapping program (Johnson et al. 2017), but we classified areas of unmapped nearshore zone separately using auxiliary data sources. Specifically, we simplified shoreline data derived from the National Oceanic and Atmospheric Administration's Environmental Sensitivity Index (https://response.restoration.noaa.gov/oil-and-chemical-spills/oil-spills/environmental-sensitivity-index-esi-maps, accessed 1 Sep 2019) to rock versus sediment categories, then we compiled the best available bathymetry, substrate, and shoreline data from the SeaGrant project (https://caseagrant.ucsd.edu/project/filling-the-white-zone-new-methods-for-interpolating-seafloor-attributes-in-californias, accessed 1 Sep 2019) and used these data to interpolate benthic substrate type and depth contours in the unmapped nearshore zone (a narrow band generally <10 m depth coastwide). We conducted interpolation between the shoreline layer and deeper benthic layers at the scale of a 30-m × 30-m grid. We interpolated the proportion of rock substrate using inverse distance weighting (with weighting of 0.5), with shoreline and offshore data inputs of mean proportion of rock in each 30-m grid cell. We interpolated depths across the unmapped zone using the natural neighbor technique in ArcGIS, with shoreline and offshore data inputs of mean depth in each 30-m grid cell. We then up-scaled the resulting GIS layers for depth (D) and proportion of rock (using bi-linear interpolation and averaging) to the common 100-m grid. Finally, because equilibrium densities within enclosed estuaries may differ from those in soft-sediment areas of the open coast (Silliman et al. 2018), we also included a categorical switch variable to identify grid cells in estuarine areas (1 for estuaries, 0 for open coast).

Another physical variable predictive of sea otter abundance is distance to shore (DS), which we computed as the Euclidean distance in meters from the centroid of each grid cell to the nearest permanently exposed shoreline (i.e., excluding emergent rocks that are covered at high tide). In general, higher densities of otters are found closer to shore (Bodkin and Udevitz 1999, Tinker et al. 2017). Because distance to shore is strongly correlated with depth, inclusion of both variables resulted in problems with model identifiability. We therefore created an index of distance to shore that was de-trended for depth, by taking the residuals from a non-linear function relating DS to D for all grid cells (g) along the California coast:

$$\log(DS_g + 1) = 1.669 \times D_g^{0.289} + 3.123. \quad (1)$$

In equation 1 we fit the numeric coefficients using maximum likelihood, and thus residuals from this equation (DSR) provide an index of relative distance to shore that is independent from depth effects: positive values indicate areas that are farther from shore than average for a given depth, whereas negative values indicate areas that are closer to shore than average for a given depth. The DSR index is related to the slope of the continental shelf in the region around each grid cell: areas with a steep benthic slope such as the Big Sur coast (Fig. 1) tend to have negative values of DSR, whereas areas with shallow benthic slope such as northern Monterey Bay tend to have positive values of DSR. We therefore expected that the DSR index would capture several potential direct and indirect effects on sea otter density. For example, benthic shelf slope could affect sea otter density and distribution by determining how concentrated or dispersed the sea otter foraging habitat is, and could also affect oceanographic processes such as primary productivity and prey recruitment. We anticipated that the effect of DSR on habitat quality for sea otters might be non-linear; thus, we computed squared index values (DSR^2) to allow for both linear or quadratic effects of relative distance to shore (de-trended for depth).

In cases of very shallow continental slopes or offshore seamounts, accessible depths may occur extremely far from shore (e.g., tens of kilometers). Radio-tagging data from field studies suggest that sea otters rarely use these far-offshore areas (Tinker et al. 2017), unless they include shallow rocky reefs with kelp canopy; this pattern may

reflect differing prey communities or lack of proximity to shelter in far-offshore areas. Regardless, to allow for an offshore effect beyond that explained by the DSR index, we calculated an offshore index (OFSH) as:

$$\mathrm{OFSH}_g = [\max(0, DS_g - 1{,}000)/5{,}000]^2 . \quad (2)$$

Equation 2 takes on values of 0 for distance-to-shore values <1,000 m, and the quadratic functional form is structured to allow that OFSH becomes substantial only at large distances from shore (≥5 km). Equation 2 is scaled using a divisor of 5,000 to produce values of the same approximate magnitude as other habitat variables, to facilitate model fitting.

In addition to the physical habitat variables described above, we also consider biotic variables that may affect habitat quality for sea otters. Kelp forests provide 3-dimensional structure over shallow rocky reefs along the California coast and support a diverse assemblage of species (Miller et al. 2018), and sea otters may preferentially use kelp forests, where prey is more abundant (Riedman and Estes 1990). We therefore created a GIS-based kelp canopy layer throughout sea otter range in California. We determined kelp forest canopy occurrence using the Landsat satellites from 1984–2018 following established methods (Cavanaugh et al. 2011, Bell et al. 2017). Briefly, we acquired Level-2 Surface Reflectance products from Landsat 5 Thematic Mapper, Landsat 7 Enhanced Thematic Mapper+, and Landsat 8 Operational Land Imager from the United States Geological Survey (https://earthexplorer.usgs.gov, accessed 1 Sep 2019). We used a binary decision tree classifier to classify each 30-m × 30-m pixel as seawater, cloud, land, or kelp canopy for each image date. We retained all pixels classified as kelp canopy in ≥1% of the Landsat images to minimize errors of omission. We validated classifications by comparing the binary decision tree classifications to manual classifications of kelp canopy area (Bell et al. 2020). We then generated an annual time series of kelp canopy occurrence in each pixel and determined the proportion of years in which a pixel contained kelp canopy. We up-scaled these relative kelp presence values (using bi-linear interpolation and averaging) to the 100-m grid cells.

Another biotic variable likely to affect sea otter abundance is the overall productivity (recruitment and growth rates) of key invertebrate prey species. Spatially explicit data on most sea otter prey species are not available; we therefore used the Vertically Generalized Production Model (VGPM; https://www.science.oregonstate.edu/ocean.productivity, accessed 1 Sep 2019) of net primary production (NPP) as a proxy index for spatial differences in mean invertebrate productivity. The VGPM model estimates net primary production from remotely sensed chlorophyll concentrations using temperature-dependent photosynthetic efficiency at a spatial resolution of 9 km (Behrenfeld and Falkowski 1997). Primary productivity derived from this dataset has been positively correlated with populations and habitat selection of other top predators such as reef sharks and dolphins (Nadon et al. 2012, Huang et al. 2019), the quantity of food delivered to macroinfaunal communities (Campanyà-Llovet et al. 2018), and the growth and recruitment of rockfishes (*Sebastes* spp.) to coastal areas (Wheeler et al. 2017). We generated the mean monthly net primary production from 2002–2018 for subtidal areas along the coast of California as a proxy for ecosystem productivity, and interpolated values at each grid cell centroid. We then centered and re-scaled values of NPP, to produce index values for each grid cell ($\mathrm{NPP}i_g$) of the same approximate magnitude as other habitat variables and thus facilitate model fitting:

$$\mathrm{NPP}i_g = (\mathrm{NPP}_g - 3{,}000)/1{,}000. \quad (3)$$

State-Space Model

We designed a dynamic population model with the goal of estimating carrying capacity (K) of sea otters at multiple spatial scales. To accomplish this goal, we used Bayesian methods to fit a state-space model in which the abundance of otters (N) varies across years within designated coastal sections, with dynamics determined by a density-dependent (theta-logistic) process model. In addition to density-dependent mortality, the process model also incorporates year-to-year stochastic variation in mortality (i.e., temporally induced environmental stochasticity), additional non-density-dependent mortality due to shark bites (Tinker et al. 2016), and positive effects on recruitment associated with an unusual pulse in the abundance of urchins and mussels in some areas of the coast after 2013 (Carr and Caselle 2018). By fitting the process model to 3 observed data sets ($C_{s,t}$, O_g, $Z_{sb,s,t}$, and $Z_{s,t}$), we derived local and regional estimates of K and the parameters of a function relating K to the habitat variables described above. We then applied the function to the entire historical range in California, and thus forecast the probable values of K for currently unoccupied areas of the coast.

Process model.—We quantified sea otter density in units of independent otters/km^2 of habitat; we excluded dependent pups for the purpose of tracking across-year variation in abundance because it reduces the effects of statistical noise associated with pup counts, which can vary year to year based on kelp canopy conditions, timing of pupping, and other factors. Our goal was to estimate the density of sea otters at carrying capacity, which we represent using the symbol κ to differentiate this density-based metric from K, the absolute number of otters that can be sustained at equilibrium within a specified area. We assumed that the expected density at carrying capacity for any grid cell g along the open coast (κ_g) can be computed as a log-linear function of a suite of local habitat variables:

$$\log(\kappa_g) = \alpha_0 + \sum_j \alpha_j H_{j,g} + f\,(D_g \mid \beta_1, \beta_2, D^*) + \zeta_{s(g)}, \quad (4)$$

where α_0 represents mean log density in soft-sediment areas of the open coast, the second term represents the net effects of all habitat variables ($H_{j,g}$) evaluated at grid cell g, the third term is a function describing the effect of depth at

grid cell g, and $\zeta_{s(g)}$ is a random effect representing the unexplained deviation from expected density for grid cells occurring in the coastal section s that contains grid cell g distributed as a random normal variate with mean of zero and standard deviation (σ_k) to be estimated. Because equation 4 is log-linear, the multipliers of each habitat variable (α_j) can be interpreted as log-ratios (i.e., the log of the proportional increase [for positive values of α_j] or decrease [for negative values of α_j] associated with a unit change in the associated habitat variable H_j). The habitat variables we considered included the proportion of substrate composed of rock, relative kelp canopy presence, occurrence of estuarine areas, the distance to shore index de-trended for depth (DSR and DSR^2), offshore effects (OFSH), and the index of net primary productivity (NPPi). In the case of water depth (D), previous researchers reported a non-linear functional relationship between otter density and depth, such that the highest densities occur at some intermediate depth and densities decrease inshore and offshore from this modal depth (Tinker et al. 2017). To accommodate this non-linearity, the effect of depth in equation 4 is described as a non-linear function:

$$f(D_g \mid \beta_1, \beta_2, D^*) = -0.01 \times [\beta_1 \times \max(0, D^* - D_g)^2 + \beta_2 \times \max(0, D_g - D^*)^2], \quad (5)$$

where the modal depth (D^*) represents the depth associated with the highest sea otter densities and the β parameters determine the rate of decrease in otter density as depths decrease (β_1) or increase (β_2) relative to the modal depth. Evaluating equations 4 and 5 provided the expected local equilibrium density (κ_g) at any location in open coastal areas.

We multiplied expected equilibrium cell densities (κ_g) by grid cell area ($A_g = 0.01\,\text{km}^2$) and then summed across all grid cells within a coastal section (Fig. 1) to obtain an estimate of K_s, the estimated abundance at carrying capacity for coastal section s. We used the estimated value of K_s to model density-dependent population dynamics using a recursive theta-logistic growth equation, whereby the number of independent otters in section s at year t ($N_{s,t}$) is calculated as:

$$N_{s,t} = N_{s,t-1} \times \exp(r_{\max}(1 - [N_{s,t-1}/K_s]^\theta) - \delta_{s,t} + \upsilon_{s,t} + \varepsilon_{s,t}). \quad (6)$$

In addition to K_s, equation 6 includes parameters that determine the maximum rate of growth at low densities ($r_{\max}$), the rate at which growth rates decline as populations increase (θ, where $0 < \theta < \infty$ and $\theta = 1$ corresponds to simple logistic growth), density-independent mortality from shark bite ($\delta_{s,t}$), positive effects on recruitment associated with the urchin abundance pulse after 2013 ($\upsilon_{s,t}$), and unexplained environmental stochasticity ($\varepsilon_{s,t}$), assumed to be distributed as a random normal variate with mean of 0 and standard deviation (σ_r) to be estimated. To account for temporally and spatially autocorrelated variation in shark-bite mortality (Tinker et al. 2016), we incorporated a conditional autoregressive (CAR) model (Besag 1974, Banerjee et al. 2003, Gelfand and Vounatsou 2003) to describe variation in δ over s and t. We used a simple spatiotemporal CAR model (following Liu et al. 2017), which required 3 additional fitted parameters: the baseline log mortality rate (γ_0), the magnitude of spatial variation in δ (σ_δ), and the degree of temporal autocorrelation in δ (ρ; detailed methods of the CAR model formulation are available online in Supporting Information, Appendix 1). We treated the urchin pulse effect as a fitted constant (υ') applicable to a subset of coastal sections and years ($s = 7$–9 and $t > 2013$), based on previously published data (Carr and Caselle 2018), and forced to zero for all other values of s and t.

Data model.—Annual range-wide survey counts in California are assumed to be reflective of true population dynamics, but with observer error (a combination of measurement uncertainty and sampling error) tending to inflate variation in counts. Accordingly, we used a negative binomial distribution to account for overdispersion in counts relative to what would be expected for a Poisson process. We assumed the number of otters counted in s at t to be drawn from a negative binomial distribution with mean equal to the true abundance ($N_{s,t}$):

$$C_{s,t} \sim \text{Negative Binomial}\,(\bar{x} = N_{s,t}, \eta_{c,s}), \quad (7)$$

where $\eta_{c,s}$ is a shape parameter controlling the degree of overdispersion in counts (variance $= \bar{x} + \bar{x}^2/\eta_{c,s}$, smaller values of $\eta_{c,s}$ indicate higher variance). Because we expected that sections would differ with respect to the magnitude of observer error (e.g., data from sections censused using aerial methods tend to be more over-dispersed than data from sections censused by shore-based observers), we treated $\eta_{c,s}$ as a hierarchical parameter: specifically, $\log(\eta_{c,s})$ is drawn from a normal distribution with mean of $\log(\eta_c)$ and standard deviation (σ_η) to be estimated.

We used a similar approach for O_g; however, the large number of grid cells posed a computational challenge, so to facilitate model fitting we first collapsed grid cells into larger groupings of adjacent cells. We defined 100 sub-sections, or bins, for each coastal section, by dividing subtidal benthic areas into 25 contiguous bands parallel to the coast and of similar depth throughout each band, then sub-dividing each depth band into 4 equal lengths (each ~5–10 km). The depth bands were of varying width: between the shore line and the 20-m depth contour, depth bands corresponded to the area between adjacent 1-m isobaths; between 20 m and 30 m, depth bands corresponded to the area between adjacent 5-m isobaths; and between 30 m and 60 m, depth bands corresponded to the area between adjacent 10-m isobaths. We then defined an additional bin for any estuarine areas in section s. We summed the cumulative grid cell counts for all grid cells falling within a bin (b), and assumed these tallies followed a negative binomial distribution:

$$O_{b\in s} \sim \text{Negative Binomial}\left(\bar{x} = \left[\frac{\sum_{g\in b} A_g \kappa_g}{K_s}\right] \sum_t N_{s,t}, \eta_o\right), \quad (8)$$

where η_o is a shape parameter. The mean expected count for bin b in section s thus depends on the summation of total abundance across survey years, scaled by the proportion of estimated K for section s accounted for by the grid cells falling within b.

We used observed data on beach-cast carcass distributions—specifically, the ratio of shark-bitten to non-shark-bitten female carcasses—to improve model fit by estimating a separate mortality parameter ($\delta_{s,t}$) for shark-bite effects. We limited consideration to female carcasses because in sea otter populations, as with many polygynous mammals, female mortality is the primary influence on population trends (Tinker et al. 2006). We assumed that the observed number of female shark-bite carcasses in section s at year t ($Z_{sb,s,t}$) is drawn from a binomial distribution:

$$Z_{sb,s,t} \sim \text{Binomial}(\text{probability} = \hat{R}_{s,t}, \text{count} = Z_{s,t}), \quad (9)$$

where $Z_{s,t}$ represents the number of female carcasses recovered in s at t and where the expected probability that a carcass is shark-bitten ($\hat{R}_{s,t}$) is calculated as:

$$\hat{R}_{s,t} = \frac{1 - \exp(-\delta_{s,t})}{1 - \exp(-d_{\min} - r_{\max}((N_{s,t}/K_s)^{\theta}) - \delta_{s,t})}. \quad (10)$$

The numerator of equation 10 describes *per capita* annual deaths attributable to shark bites, and the denominator describes total *per capita* deaths from all sources of mortality. The denominator includes a parameter describing the instantaneous death rate for adult female sea otters ($d_{\min}$) in a population growing at or near $r_{\max}$, which we set to 0.048 based on previously published analyses (Tinker et al. 2019*b*).

Model fitting and evaluation.—The observed data variables ($C_{s,t}$, O_g, $Z_{sb,s,t}$, $Z_{s,t}$) constrain the possible values of unknown parameters in the process model (α_0, α_j, β_1, β_2, D^*, r_{max}, θ, ρ, γ_0, υ', σ_k, σ_r, σ_δ) and observer model (η_o, σ_η, η_o), allowing us to estimate posterior distributions for these parameters using standard Markov chain Monte Carlo (MCMC) methods. We used vague prior distributions for most parameters (i.e., weakly informed based on biological feasibility but having no information specific to the analysis), including Cauchy priors for fixed-effect parameters in equations 4 and 5, half-Cauchy priors for all variance and dispersion parameters (Gelman 2006, Gelman et al. 2008), and gamma priors for D^* and θ (Table 1). For $r_{\max}$ we used a strongly informed normal prior with mean of 0.2 and standard deviation of 0.05, reflecting the results of multiple studies showing that $r_{\max}$ consistently falls within this range for sea otter populations (Jameson et al. 1982, Estes 1990, Monson et al. 2000, Gerber et al. 2004, Lafferty and Tinker 2014). We used R (R Core Team 2014) and Stan software (Carpenter et al. 2017) to code and fit the model, saving 20,000 samples after a burn-in of 5,000 samples. We evaluated model convergence by graphical examination of trace plots from 20 independent chains and by ensuring that the Gelman-Rubin convergence diagnostic (psrf) was ≤1.1 for all fitted model parameters. To validate the model and evaluate goodness of fit, we conducted posterior predictive checking, using the χ^2 statistic (sum of squared Pearson residuals of annual survey counts and grid cell cumulative counts vs. expected values) to compare fit of observed data and new data (i.e., out of sample observations) generated from the same distributions (Gelman et al. 2000). We examined scatter plots of the posterior distribution of χ^2 scores for new versus observed data (in the case of well-fitting models, points in such a plot should be evenly distributed around a line with slope of unity and zero intercept) and we used the χ^2 scores to compute the Bayesian P value (the proportion of out of sample observations more extreme than existing observations; Gelman 2005, Ghosh et al. 2007), which should fall within the range of 0.2–0.8 for a well-fit model. We summarized model results by reporting the mean and 95% credible interval (CrI) of parameter posterior distributions. We included habitat variables in the final model if their 95% CrI did not include zero, and we compared the full model to reduced models using the leave-out-one information criterion to assess relative model support (Vehtari et al. 2017). Additionally, we calculated the unexplained variance in observed local densities for each model (i.e., mean squared deviations from expected densities given the fixed effects included in eq. 4). We calculated unexplained variance by summing ${\sigma_k}^2$ and the variance associated with the negative binomial distribution of grid cell counts ($\bar{x} + \bar{x}^2/\eta_o$, where $\bar{x} = exp(\alpha_0)$). We then calculated the proportional reduction in unexplained variance relative to a null model (i.e., intercept only) or a model having only an intercept and depth effects; this allowed us to assess the degree to which inclusion or exclusion of different variables affected the amount of variation explained by the model.

Range-Wide Projections of *K* and a Candidate Value for OSP in California

For the 20 coastal sections within the currently occupied range (the central coast and San Nicolas Island; Fig. 1), fitting the state-space model provided point estimates of K_p and associated uncertainty (described by the 95% CrI of the posterior distributions). We report densities at carrying capacity (κ) for coastal sections, standardized to mean otters/km^2 of habitat between 0–40-m depth, to facilitate comparison with previously reported density values (Laidre et al. 2001). We evaluated fine-scale spatial variation in κ within the current range by plotting the coastal 100-m grid with cells color-coded by the model-estimated values of κ_g. In the case of currently unoccupied areas of the coast, we generated posterior predictive distributions of κ_g by iteratively drawing from posterior distributions for all model parameters and evaluating equations 4 and 5. Summing these predictive distributions of κ_g multiplied by grid areas (A_g), we calculated point estimates and 95% CrI of K for

Table 1. Summary of parameters used in a state-space model of southern sea otter population dynamics, California, USA, 1983–2018, in which mean density at carrying capacity (derived parameter κ) is estimated as a function of local habitat variables. We provide a brief description of each parameter, the Bayesian prior distribution, and the mean, standard deviation, and 95% credible interval (CrI) of the fitted posterior distribution. We also show the effective sample size for estimation of each parameter (n_{eff}) and the potential scale reduction factor (psrf), which measures convergence (chain mixing) for each parameter, with values close to 1 indicating good convergence. Parameters for Cauchy and half Cauchy distributions include the location parameter (a) and scale parameter (b).

Parameter	Description of parameter	Prior distributions	$\bar{x}$	SD	Lower CrI	Upper CrI	n_{eff}	psrf
α_0	Intercept of function predicting κ based on habitat variables; represents mean log-density in soft-sediment outer coast	Cauchy(a = 0, b = 2.5)	0.8024	0.3266	0.2095	1.4980	4,050	1.003
D^*	Modal depth (the depth at which average densities are highest)	Gamma($\bar{x}$ = 10, SD = 5)	5.6920	0.7253	4.2920	7.1090	15,620	1.000
β_1	Effect on κ of varying depth, moving inshore from D^*	Cauchy(a = 0, b = 2.5)	3.6510	1.4520	1.6750	7.1430	13,850	1.000
β_2	Effect on κ of varying depth, moving offshore from D^*	Cauchy(a = 0, b = 2.5)	0.1274	0.0073	0.1132	0.1421	16,880	1.000
α_{EST}	Effect on κ of estuarine areas (relative to soft-sediment open coast)	Cauchy(a = 0, b = 2.5)	1.4360	0.5325	0.2906	2.3660	10,730	1.001
α_{PR}	Effect on κ of increasing proportion of rocky substrate	Cauchy(a = 0, b = 2.5)	1.7070	0.1352	1.4420	1.9690	26,050	1.000
α_{PK}	Effect on κ of increasing frequency of kelp presence	Cauchy(a = 0, b = 2.5)	2.5830	0.1504	2.2880	2.8730	25,120	1.000
α_{DSR}	Effect on κ of deviations from mean slope, linear response	Cauchy(a = 0, b = 2.5)	0.1931	0.0926	0.0075	0.3719	19,040	1.000
α_{DSR2}	Effect on κ of deviations from mean slope, quadratic response	Cauchy(a = 0, b = 2.5)	0.2074	0.0625	0.0817	0.3250	22,410	1.000
α_{OFSH}	Effect on κ of increasing distance from shore beyond 1 km (i.e., far offshore effect)	Cauchy(a = 0, b = 2.5)	−0.5990	0.1722	−0.9361	−0.2614	21,640	1.000
α_{NPP}	Effect on κ of increasing index of net primary productivity	Cauchy(a = 0, b = 2.5)	0.5381	0.1281	0.2864	0.7903	23,290	1.000
$r_{\max}$	Max. rate of population growth at low densities	Normal($\bar{x}$ = 0.2, SD = 0.05)	0.1777	0.0190	0.1449	0.2188	3,717	1.005
θ	Shape parameter in theta-logistic growth model, affects response of growth to density changes	Gamma($\bar{x}$ = 1, SD = 0.5)	0.8744	0.2598	0.4694	1.4640	3,361	1.006
υ'	*Per capita* effect of prey glut for segments (s) = 7–9, t > 2013	Cauchy(a = 0, b = 0.5)	0.1838	0.0479	0.0912	0.2796	12,330	1.001
η_o	Dispersion parameter for negative binomial distribution of summed counts in grid cells	Half Cauchy(a = 0, b = 2.5)	0.8251	0.0305	0.7664	0.8859	32,180	1.000
η_c	Mean dispersion parameter for negative binomial distribution of annual counts in coastal segments	Half Cauchy(a = 0, b = 2.5)	12.8100	6.1750	4.9300	28.1800	12,790	1.000
σ_η	Magnitude of random variation in the log of η_c among coastal segments	Half Cauchy(a = 0, b = 2.5)	1.8350	0.3754	1.2500	2.7250	9,873	1.002
σ_k	Magnitude of random variation in log-density at K among coastal segments	Half Cauchy(a = 0, b = 2.5)	0.9343	0.2769	0.4800	1.5610	3,098	1.005
σ_r	Magnitude of random variation in *per capita* growth rates (environmental stochasticity)	Half Cauchy(a = 0, b = 2.5)	0.1006	0.0159	0.0707	0.1323	413	1.048
σ_δ	Magnitude of spatial variation in log of conditional auto-regressive parameter δ	Half Cauchy(a = 0, b = 2.5)	0.0941	0.0374	0.0405	0.1833	250	1.087
ρ	Temporal correlation in log of conditional auto-regressive parameter δ	Beta(a = 1, b = 1)	0.9313	0.0381	0.8455	0.9921	459	1.045
γ_0	Baseline log of mortality rate from shark bite	Cauchy(a = 0, b = 2.5)	−3.9340	0.5142	−5.0620	−3.0400	2,703	1.008
$\delta_{1,2010}$	*Per capita* effect of shark-bite mortality, example 1 (s = 1, t = 2010)	NA (CAR model)	0.2293	0.1027	0.0809	0.4815	13,890	1.001
$\delta_{17,2010}$	*Per capita* effect of shark-bite mortality, example 2 (s = 17, t = 2010)	NA (CAR model)	0.3500	0.1386	0.1395	0.6768	6,285	1.002

4 currently unoccupied coastal regions—the North coast (Oregon border to Pigeon Point), San Francisco Bay, South coast (Gaviota State Park to the Mexico Border), and the Channel Islands (Fig. 1)—and a range-wide estimate of K for all possible sea otter habitat in California. We report 2 metrics for abundance values: independent otters only (excluding dependent pups) and independents plus pups (calculated using an empirically derived average pup:adult ratio of 0.15; Tinker and Hatfield 2017).

In addition to local and regional estimates of K, an important metric for management of marine mammal populations under the MMPA is the OSP, operationally defined as an abundance level that falls between maximum net productivity level (MNPL) and K (Gerrodette and DeMaster 1990). Various guidelines have been suggested for setting OSP, including incorporation of uncertainty in population status and demographic parameters (Taylor et al. 2000). By fitting the state-space model, we obtained point estimates and associated uncertainty measures for K and the other key parameters of a theta-logistic population growth model (eq. 6). We used these values to estimate an appropriate candidate value for OSP that accounted for uncertainty in all relevant parameters. For each coastal section within the current defined range (Fig. 1), we solved 10,000 iterations of equation 6 in which we randomly selected parameter values from their joint posterior distributions (but with $\delta_{s,t}$ and $\upsilon_{s,t}$ forced to zero). For each iteration we systematically varied $N_{s,t-1}$ over a sufficiently large range of values that should include the highest expected net growth (between 20% and 80% of the point estimate of K_s), then numerically solved for the abundance value associated with the maximum growth rate (calculated as the difference between $N_{s,t}$ and $N_{s,t-1}$); this value of $N_{s,t-1}$ represented the MNPL point estimate associated with a specific combination of parameter values. We calculated the upper quartile of the resulting distribution of iterated MNPL estimates, which we suggest as an appropriate candidate value for a local OSP (OSP_s) because this accounts for demographic processes and parameter uncertainty. Finally, we summed OSP_s across sections within each of the 5 regions to obtain regional OSP values, and across regions to arrive at a California-wide candidate value for OSP.

RESULTS

The state-space model provided a good fit to observed data (Bayesian $P = 0.462$; Fig. S2, available online in Supporting Information) and MCMC chains converged well, with all psrf values <1.1 (Table 1). The estimated rate of shark-bite mortality increased over the last decade of the time series (2007–2017), with the highest values ($\delta_{s,t} \geq 0.2$) occurring near the northern and southern peripheries of the central coast range (Table 1; Fig. 2) and associated with local declines in sea otter abundance in these coastal sections after 2007 (Fig. 3A,B). We observed a contrasting trend for the Monterey Peninsula region after 2013, where positive effects on *per capita* recruitment ($\upsilon' = 0.18$; Table 1), apparently due to a glut of urchin and mussel prey (Carr and Caselle 2018), were associated with a localized increasing trend in sea otter abundance (Fig. 3C,D). The posterior estimates of $\delta_{s,t}$ and υ, together with estimates of K_s, $r_{\max}$, θ, and σ_r (Table 1), resulted in predicted population dynamics that were in good agreement with observed survey counts (Fig. 3A–E).

The best-supported model for predicting K included all habitat variables (Table 2), each of which was statistically significant (Table 1; Fig. S3, available online in Supporting Information). Inclusion of habitat variables reduced unexplained variance in grid cell counts by almost half (42%) as compared to an intercept-only model, or by 17% as compared to a depth-only model (Table 2). Depth had a strong effect on sea otter density, with the highest

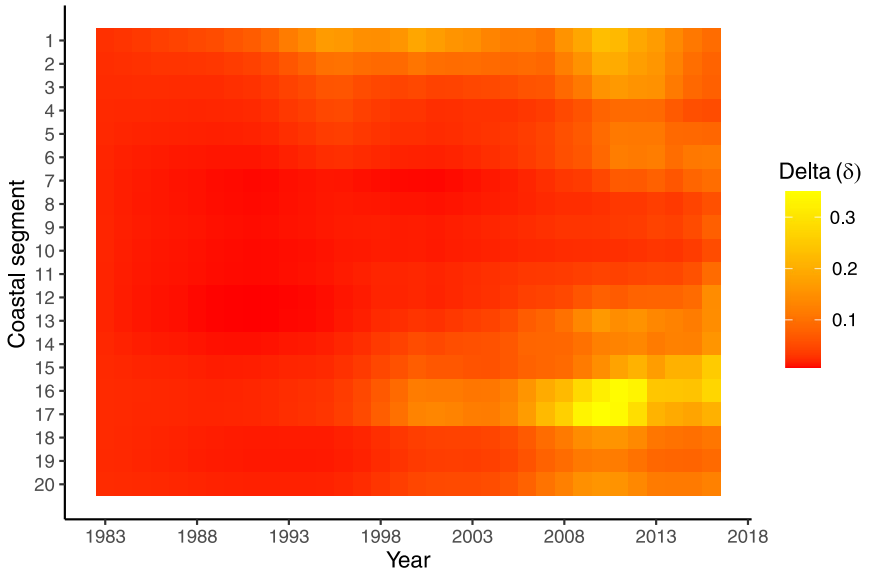

Figure 2. Heatmap plot in which color intensity represents the estimated magnitude of delta ($\delta_{s,t}$), the instantaneous rate of shark-bite mortality for sea otters in any given year (horizontal axis) and coastal section (vertical axis) of California, USA, 1983–2018.

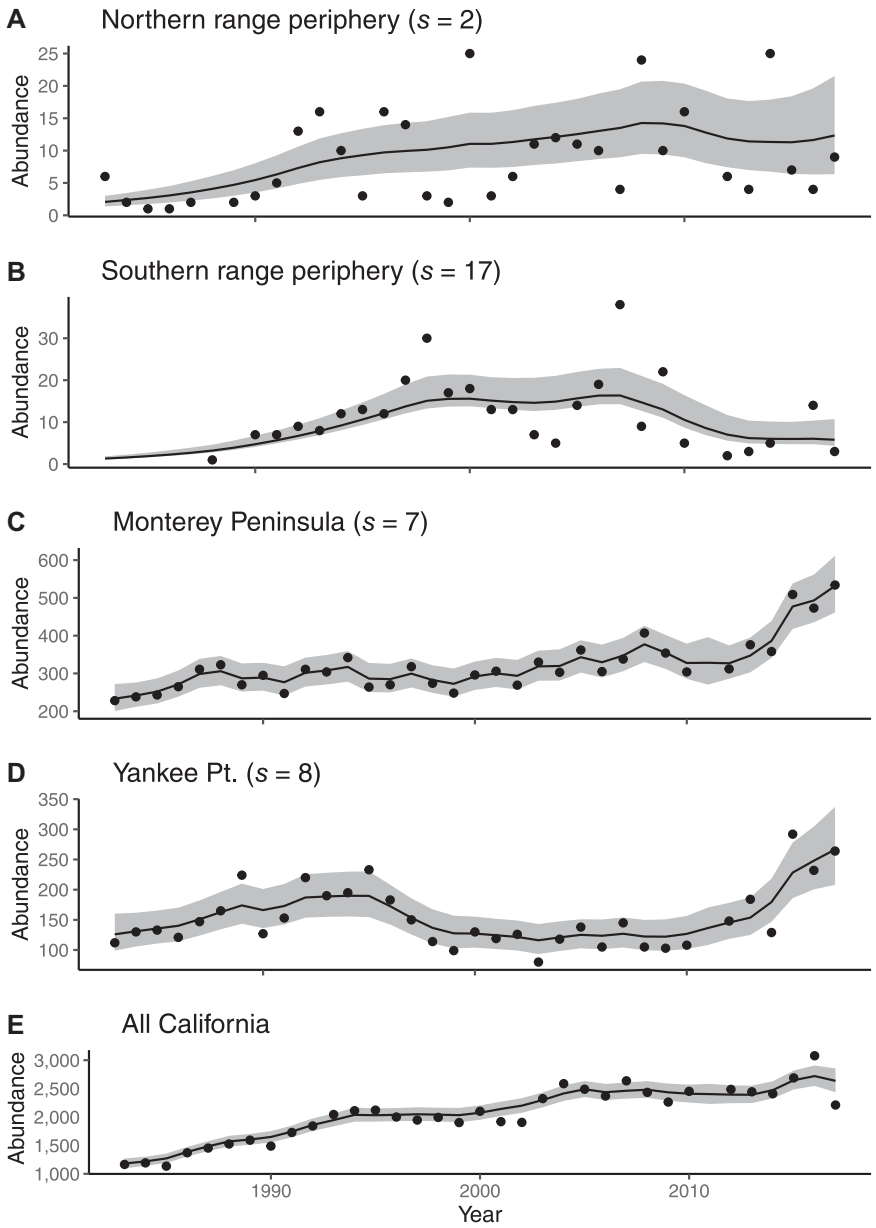

Figure 3. Observed survey counts (points) and model-estimated trends (black lines), together with 95% credible intervals (CrI; gray shaded bands), of sea otter abundance in coastal California, USA, 1983–2018. Trends are plotted for 4 of the 20 coastal sections (*s*; panels A–D) and for all currently occupied areas of California (panel E).

equilibrium densities occurring between 3 m and 20 m of depth ($D^* = 5.7$, 95% CrI = 4.29–7.11) and declining densities inshore and offshore of this range (Fig. 4A). Estuarine areas supported higher equilibrium densities, on average, than did soft-sediment areas of the outer coast; the mean density at *K* in estuaries was 9.38 otters/km^2 (95% CrI = 1.64–47.65) as compared to 2.23 (95% CrI = 1.23–4.47) in equivalent coastal soft-sediment areas. Benthic substrate composition had a strong effect, with rocky areas supporting higher densities than soft-sediment areas, and an increase in the proportion of rocky substrate from zero to 50% resulting in more than a doubling of the mean density at *K* (Fig. 4B). The presence of kelp canopy was associated with higher densities as well; an area with 50% kelp cover supported 3.6 times more otters at *K* than an equivalent area without kelp canopy (Fig. 4C). Areas of high NPP supported more otters; an NPP value of 4,000 was associated with equilibrium densities 1.5 times higher than the average NPP value of 3,000 (Fig. 4D). There was a non-linear relationship between density at *K* and the slope of the benthic shelf, with higher densities predicted in areas with shallower-than-average slopes and areas with steeper-than-average slopes (Fig. 4E). Finally, areas that were far offshore supported much lower densities than nearshore areas; the mean density in an area 10 km from shore was just 17% (95% CrI = 4.9–42.8%) of the mean density in an area 1 km from shore having identical substrate and depth.

Table 2. Comparison of relative support for alternative models used to estimate local carrying capacity (K) for southern sea otters, California, USA, 1983–2018. Model support is measured using information-theoretic methods, with lower values of the leave-out-one information criterion (LOOic) indicating better support. We also provide standard errors for LOOic estimates. We show the standard deviation parameter (σ_k) for unexplained variation in the density at K among coastal sections, and the negative binomial dispersion parameter (η_o) for grid cell counts (higher values indicate lower dispersion) for each model. Combining these variance components, we present the overall residual variance (variation in counts around model-predicted values). We then calculated the proportional reduction in residual variance of each candidate model relative to a reduced model that includes only an intercept and depth effects, and a null model in which only an intercept is included.

						Variance reduction	
Model	**LOOic**	**SE**	σ_k	η_o	**Variance**	**vs. depth**	**vs. null**
Full model	14,325.3	167.6	0.904	0.8251	7.3760	16.95%	42.40%
No estuary effect	14,326.9	167.3	1.216	0.8204	8.0631	9.21%	37.03%
No NPP[a] effect	14,331.1	166.5	0.890	0.8201	7.3793	16.91%	42.37%
No offshore effect	14,337.8	168.6	0.914	0.8201	7.4218	16.44%	42.04%
No distance to shore effect	14,341.5	169.7	0.951	0.8172	7.5074	15.47%	41.37%
No kelp effect	14,465.0	172.6	0.829	0.7594	7.6437	13.94%	40.31%
No rocky substrate effect	14,549.2	173.4	0.695	0.7216	7.7028	13.27%	39.85%
Depth-only model	14,827.5	187.1	0.891	0.6195	8.8815		30.64%
Null model (intercept only)	15,686.7	195.3	1.087	0.3931	12.8053		

[a] NPP = net primary productivity.

The combined influence of habitat variables and random effects resulted in considerable spatial variation in estimated density at K at the scale of coastal sections, ranging from >10 otters/km^2 around Monterey Peninsula ($s = 7$) and Elkhorn Slough estuary ($s = 5$) to <1.5 otters/km^2 in sandy embayments such as northern Monterey Bay ($s = 4$; Fig. 5A). Evaluating equation 4 for all grid cells resulted in map-based projections of fine-scale variation in equilibrium densities (Fig. 5B). We applied these fine-scale projections to both occupied and currently unoccupied habitats throughout California (Fig. S4, available online in Supporting Information); the resulting maps provide a means to identify potentially important future habitat areas for sea otters. Summing across all grid cells, we obtained projected abundance at K for 5 regions within California (Fig. 6; Table 3), which when tallied produced a California-wide estimate of 17,226 otters (95% CrI = 9,739–30,087, including both independents and dependent pups). After accounting for parameter uncertainty and using simulations of theta-logistic population dynamics to examine variation in MNPL estimates, our results indicated a candidate value for OSP (for all of CA) of 10,236, which represents 59.4% of projected K. Regional OSP values ranged from 1,269 for the Channel Islands to 2,528 for the central coast (Table 3).

DISCUSSION

Estimates of potential future abundance and distribution of recovering carnivore populations can help resource managers set realistic management targets, anticipate ecosystem and possible socioeconomic changes, and identify key habitat areas for protection. The analyses we present here demonstrate that, in the case of southern sea otters, readily available geospatial data on biotic and abiotic habitat variables can be used to estimate equilibrium densities at multiple spatial scales. By estimating the functional relationships between these habitat variables and K, we developed a mechanistic understanding of how various habitat features affect spatial variation in equilibrium densities. Our results provide a means of predicting future population potential, within the current distribution and in areas where sea otters have yet to recover. Our model also provides an update to previous estimates of southern sea otter carrying capacity (DeMaster et al. 1996, Laidre et al. 2001) using a broader suite of habitat variables and more extensive and updated abundance data. By modeling dynamics using a stochastic theta-logistic process model and including density-independent mortality terms, our results provide new insights into the functional form of density dependence, the magnitude of environmental stochasticity, and spatiotemporal variation in emerging mortality sources such as shark bite.

Estimates of K for mammalian species often benefit from incorporation of data on habitat quality or prey abundance (Potvin and Huot 1983, Hobbs and Swift 1985, Iijima and Ueno 2016). Habitat variables considered should ideally relate to the demographic and ecological processes that regulated abundance, via their effects on *per capita* reproduction and survival (Hobbs and Swift 1985). Previous estimates of K for sea otters have incorporated habitat differences to improve predictions (Laidre et al. 2001, 2002; Gregr et al. 2008). Our analyses build on these earlier analyses in several important ways. First, we use a more extensive and spatially explicit set of habitat variables, including physical parameters (e.g., depth, benthic substrate composition, distance from shore) and biotic variables (e.g., kelp presence, primary productivity). All these variables were selected based on *a priori* inferences about their effects on sea otter foraging success and, ultimately, survival and productivity. By including a broad suite of continuous variables, rather than just 1 or 2 categorical variables, we were able to explain a higher proportion of the observed variation in sea otter abundance (Table 3). The incorporation of depth as a continuous variable in our model was particularly important because it allowed for different areas of the coast supporting differing numbers of otters simply based on their unique bathymetric profiles. This strong effect of depth

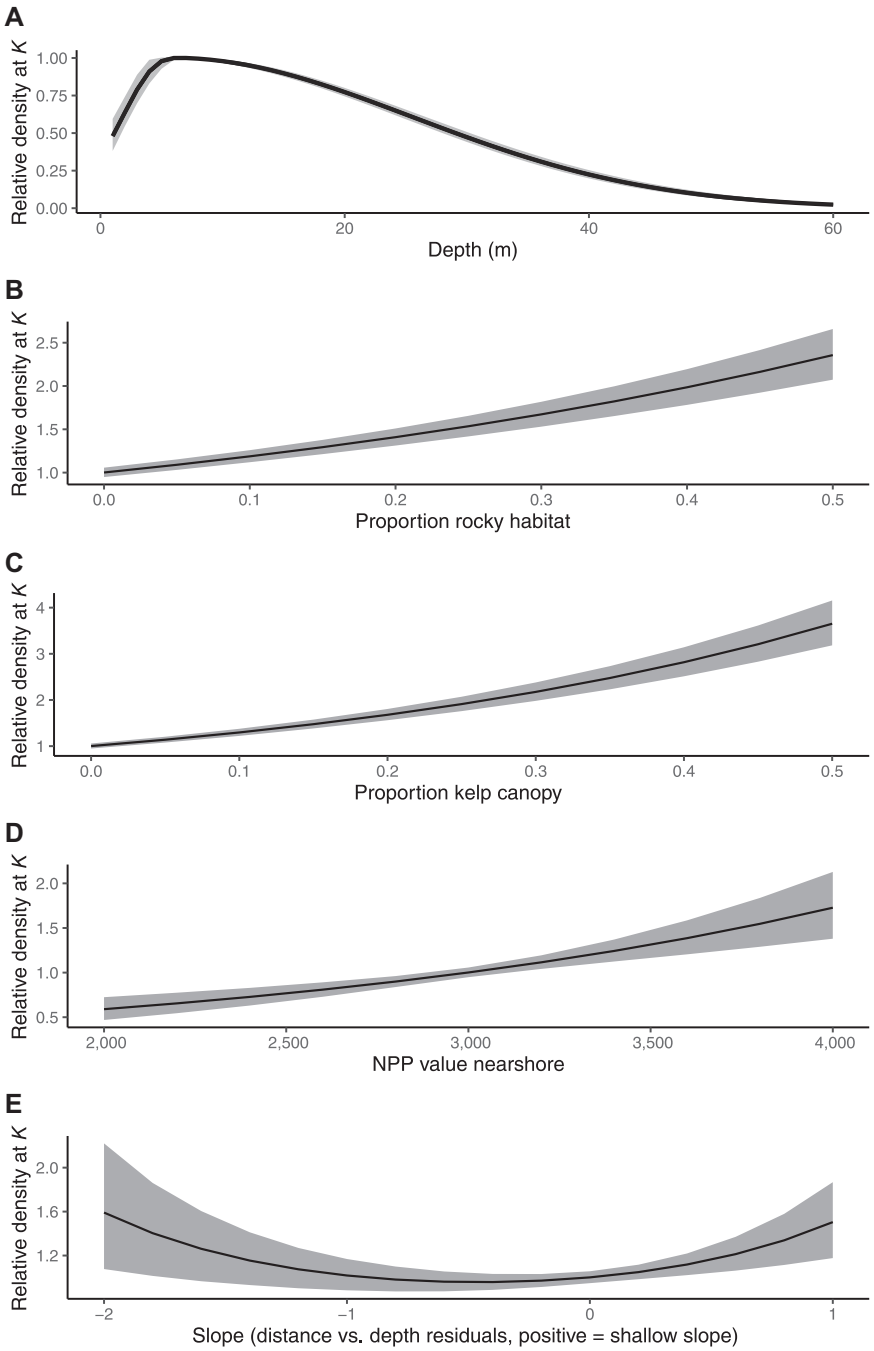

Figure 4. Plots showing the model estimated effects of 5 habitat variables on the relative abundance of sea otters at carrying capacity (K), based on survey data from coastal California, USA, 1983–2018. Habitat variables include A) the effect of depth, showing peak abundance occurring at approximately 5 m; B) proportion of benthic substrate composed of rock, with higher densities occurring in more rocky areas; C) proportional occurrence of kelp canopy, with higher densities occurring in areas having more kelp canopy cover; D) net primary productivity (NPP), with higher densities occurring in areas having higher values of NPP; and E) residuals from a function of distance to shore versus depth (DSR), whereby areas with positive residuals (i.e., farther from shore than average for a given depth, indicating shallow benthic slope) or very negative residuals (i.e., closer to shore than average for a given depth, indicating steep benthic slope) both show higher densities at K than areas of average benthic slope.

likely reflects the depth dependence of most sea otter prey species (Bodkin et al. 2004, Thometz et al. 2016). The type of substrate (rock vs. soft sediment) and kelp presence also provided key information that improved predictive power, likely reflecting the strong relationship between kelp forests and invertebrate productivity (Miller et al. 2018). Our results indicate that spatially explicit consideration of multiple habitat features can provide a better understanding of variation in sea otter equilibrium abundance, as has also been shown for terrestrial species (Iijima and Ueno 2016).

Another key feature of our model is that the state-space analytical approach does not require simplifying or subjective decisions about which areas of the coast are already at K (Buckland et al. 2004, Clark and Bjørnstad 2004, Chaloupka and Balazs 2007, Wang 2007). Indeed, all survey data are used to fit the model and thus estimate K,

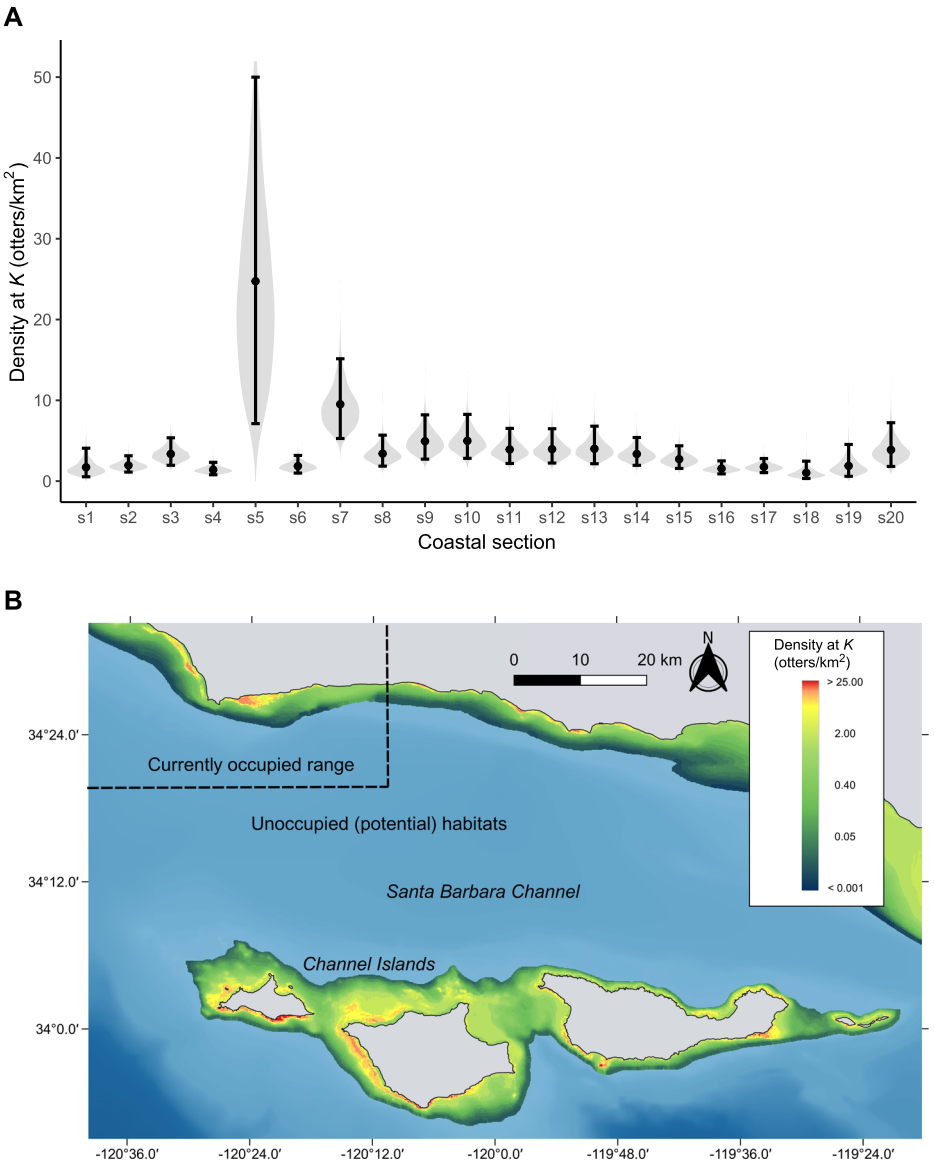

Figure 5. A) Violin plots of estimated density of sea otters at carrying capacity (K) for 20 coastal sections in central California, USA, 1983–2018. The width of the gray shaded bands illustrates the degree of model support for a given value, and the error bars span the 95% credible intervals (CrI) for the estimates. B) The Santa Barbara Channel area, with sea otter habitat in the nearshore zone color-coded to show fine-scale variation in the estimated potential density at K. The model facilitated estimates of K for both currently occupied and future potential habitats.

irrespective of their status with respect to K, the only requirement being a sufficiently long time series of counts (Wang 2009). By fitting the state-space model using Bayesian methods, we obtained realistic estimates of the uncertainty associated with each model parameter and the combined uncertainty around derived parameters such as area-specific values of K. This resulted in somewhat wider credible intervals associated with our regional and range-wide projections of K as compared to previous estimates of K (DeMaster et al. 1996, Laidre et al. 2001). We believe this represents a benefit of our modeling approach because our estimates explicitly incorporate sources of uncertainty that were not included (or not recognized) in previous analyses, including unexplained spatial heterogeneity in habitat-based relationships (described in our model by σ_k), observer error inherent in census-based estimates of abundance and trends, and the uncertainty around estimates of long-term equilibria for any given location imposed by the effects of environmental stochasticity.

Despite the differences in analytical approach between our model and previous estimates of sea otter carrying capacity, the predictions of range-wide K were strikingly similar: 17,226 otters (this study) versus 15,941 in Laidre et al. (2001) and 13,515 in DeMaster et al. (1996). This similarity in overall estimates of K is encouraging, especially given that they were arrived at using different methods and data sets, which probably reflects the consistency of demographic processes in sea otter populations (Eberhardt 1995, Monson et al. 2000, Gerber et al. 2004, Tinker et al. 2019*a*). The higher estimate from the current analysis may reflect the

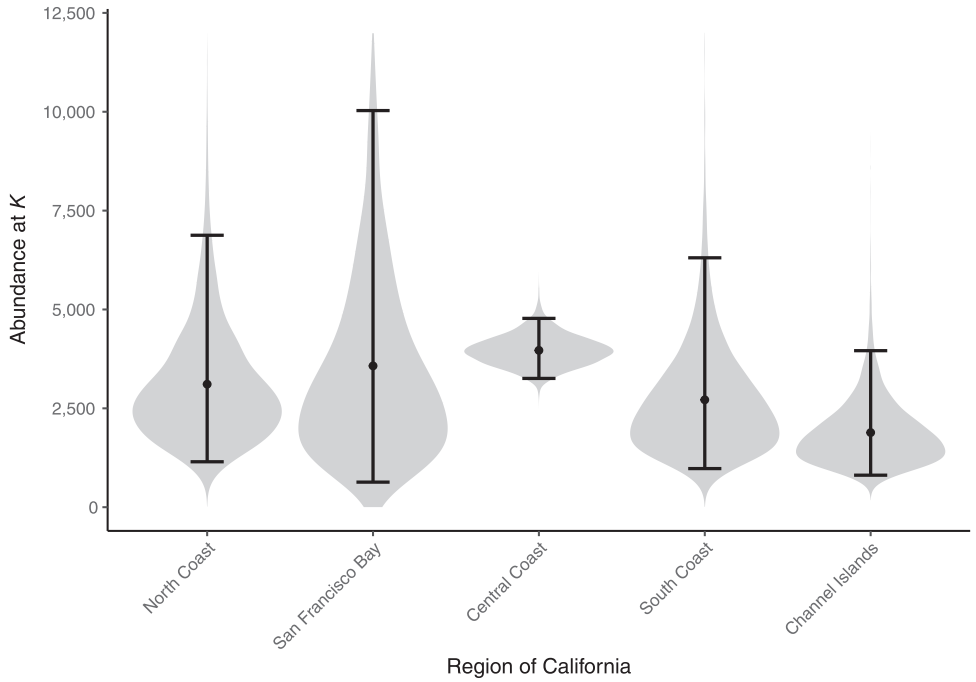

Figure 6. Violin plots showing the projected abundance at carrying capacity (K) for sea otter populations in 5 coastal regions of California, USA, 1983–2018. The width of the gray shaded bands illustrates the degree of model support for a given value, and the error bars span the 95% credible intervals (CrI) for the estimates.

more detailed treatment of habitat variation, including the differentiation of estuarine systems from outer coast soft-sediment areas (Hughes et al. 2013), and also the state-space approach, which avoids assumptions about whether index areas have already achieved K. Another similarity between our results and previous analyses is the pattern of higher equilibrium densities in rocky versus soft-sediment areas (Laidre et al. 2001), a pattern that likely reflects more productive epibenthic prey communities in rocky substrate areas. Our results reveal some further details about this relationship. First, the relative degree of kelp canopy in rocky areas provides even more information about potential densities, and second, it appears that soft-sediment estuaries can support higher densities of otters than can soft-sediment outer coast areas. A key difference between our model and previous analyses is that our model provides fine-scale and spatially explicit projections of expected K in future potential habitats (Fig. 5B), thereby providing a useful tool for resource managers to help identify key areas for conservation and management (Fig. S4). We caution that some estuarine areas outside the current range contain a diversity of substrate types, hydrological features, and human activities, and not all of these may be suitable for sea otters (Hughes et al. 2019); thus, further examination of the quality and distribution of different features within estuaries is warranted, particularly in areas modified by human activities.

An important advantage of process-based models over purely descriptive statistical models is the resulting insight into underlying mechanisms and causes of observed dynamics. Such insights are important if models are to be used for forecasting in novel conditions (Evans et al. 2012). Our state-space model features a density-dependent process model that incorporates spatial structure and environmental stochasticity and density-independent factors (shark-bite mortality, unusual prey pulses). By incorporating population structure at relevant scales, we show that the maximum rate of growth for southern sea otter populations at low density

Table 3. Estimated abundance at carrying capacity (K) and candidate values for optimal sustainable population (OSP) of southern sea otters in California, USA, 1983–2018. Estimates are listed by coastal region and as a state-wide total. We provide point estimates and 95% credible intervals (CrI) for K in units of independent otters only, and independents plus dependent pups (assuming a pup:adult ratio of 0.15). Candidate OSP values are in units of independents plus pups.

	Independents only			Independents plus pups			
Region	$\bar{x}$	**Lower CrI**	**Upper CrI**	$\bar{x}$	**Lower CrI**	**Upper CrI**	**Candidate OSP value**
North Coast	3,055	1,128	6,754	3,513	1,297	7,767	2,070
San Francisco Bay	3,509	622	9,851	4,036	716	11,328	2,527
Central Coast	3,895	3,198	4,689	4,480	3,677	5,393	2,528
South Coast	2,667	959	6,194	3,067	1,102	7,123	1,842
Channel Islands	1,853	794	3,887	2,131	914	4,470	1,269
California total	14,979	8,469	26,162	17,226	9,739	30,087	10,236

($r_{max} = 0.18$; Table 1) is almost identical to that of northern populations at low density (Tinker et al. 2019*a*). Earlier reports of much lower rates of growth for the California population (Estes 1990) were based on an unrecognized and inaccurate assumption that southern sea otters represent a single homogenous population, as opposed to a metapopulation with differing growth rates in areas of high and low density (Tinker et al. 2008, Lafferty and Tinker 2014, Tinker 2015, Davis et al. 2019). Another novel insight provided by our dynamic process model is the role of increasing shark-bite mortality in depressing population recovery or even causing local declines (Fig. 3A,B). Our results are in agreement with previous studies (Tinker et al. 2016, Nicholson et al. 2018, Moxley et al. 2019) that have reported rapidly increasing rates of shark-bite mortality at the northern and southern peripheries of the current distribution, and especially in southern areas after 2005 (Fig. 2). Whether shark-bite mortality rates will remain at these high levels or prove to be a transient phenomenon is uncertain; however, if levels remain high indefinitely, there are several implications. First, the concentration of elevated mortality near the range peripheries, where range expansion occurs (Tinker et al. 2008, Lafferty and Tinker 2014), will likely inhibit future population spread and growth in new areas. This possibility has prompted some conservation groups to suggest re-locations of stranded or rehabilitated animals to expedite range-wide recovery (Nicholson et al. 2018). Second, continued shark-bite mortality may impose a top-down-based equilibrium abundance in some areas that is lower than that dictated by prey productivity. If so, this may require re-evaluation of K to explicitly include elevated shark-bite mortality; our process-based model provides a simple way of doing this, by iterating equation 6 to numerically solve for a realized equilibrium that includes shark bite. This latter point highlights that K is not a fixed property; rather, K can change over time in response to changing conditions. Although our current analysis did not explicitly allow for temporal variation in K, such dynamics were implicit in the allowance for stochasticity in annual growth rates and shark-bite mortality, and in the relationship between K and biotic variables (kelp cover and NPP) because the biotic variables are themselves subject to temporal variation because of external forcing (e.g., the effects of climate change). Future analyses should further explore the implications of temporal variation in K.

The updated habitat-based estimate of range-wide carrying capacity, combined with the fitted parameters of a process model of sea otter population dynamics, provided a unique opportunity to estimate a candidate value of OSP for southern sea otters in California. The MMPA defines OSP as an abundance value that falls between MNPL and K (Gerrodette and DeMaster 1990). Selecting an appropriate value of OSP thus requires estimates of MNPL and K. Determining species-specific MNPL in turn requires information about demographic processes, specifically about non-linearities in the functional form of density-dependent variation in growth rates (Taylor and Demaster 1993), and failure to account for uncertainty in estimates of K and demographic parameters can result in inappropriate values of OSP (Taylor et al. 2000). We addressed both these concerns in our estimation of a candidate OSP value for sea otters by using the full range of uncertainty in the parameters of a theta-logistic growth model to obtain a distribution of credible MNPL values for each coastal section. We then took the sum of the upper quartiles of these distributions to obtain a conservative OSP candidate value for California. The upper quartile of estimates for MNPL ensures some confidence (75%) of achieving or exceeding the true MNPL and is always <80% of the point estimate for K. The candidate OSP value (10,236) corresponds to approximately 60% of the point estimate of K. Coincidentally, $0.6\,K$ is a benchmark often used to set OSP for marine mammals; however, the rationale for an OSP value falling in the range $0.5\,K$–$0.85\,K$ is the assumption that marine mammal species will generally exhibit a convex functional form of theta-logistic growth (i.e., $\theta > 1$). Although $\theta > 1$ is a reasonable assumption for most long-lived cetaceans and pinnipeds (Taylor and Demaster 1993), our fitted model for southern sea otters actually suggests a value of θ slightly below 1 (Table 1; although the 95% CrI for θ includes 1). The lower value of θ for sea otters implies that density-dependent effects on reproduction and survival emerge soon after population establishment, a pattern supported by empirical data from several recovering populations (Bodkin et al. 2000, Rechsteiner et al. 2019, Tinker et al. 2019*a*). Regardless, the reason that our candidate value of OSP is $>0.5\,K$ is not indicative of a convex functional form of density-dependent growth but rather reflects the incorporation of parameter uncertainty in our estimates of K and MNPL. Another benefit of our approach is the ability to define OSP values at smaller scales than the sub-species or stock level currently used as the basis of management (Table 3). It is increasingly recognized that management goals and objectives should ideally be set at temporal and spatial scales relevant for the species of interest (Clapham et al. 2008); in the case of sea otters, the relevant spatial scale of population regulation appears to be much smaller than the stock level, on the order of tens of kilometers (Bodkin 2015, Gagne et al. 2018, Tinker et al. 2019*a*). Unfortunately, lack of availability of comparable habitat data for Oregon and Mexico at the time of analysis prevented the application of the model to the entire historical range of the southern sea otter (USFWS 2003), but as these GIS layers become available, it will be straightforward to extrapolate projections and thus estimate candidate OSP values for these remaining areas.

The model we present for estimating K using GIS-based data on habitat variables and using state-space methods to analyze population trends, represents a powerful approach for assessing population growth potential at fine spatial scales for a recovering carnivore. The method provides new insights into habitat-density relationships and important information about the nature of density dependence, environmental stochasticity, and additional density-independent mortality. Although a similar analytical framework has been applied to terrestrial mammals (Iijima and Ueno 2016), this is a novel approach for marine mammals and could be easily

adapted for other species for which both long survey time series and detailed habitat data are available. Expanding this method to northern sea otter populations will allow comparison of habitat relationships across regions and provide insights into the habitat features or mortality sources limiting abundance in those areas. We therefore expect that our results will provide useful new tools for resource managers as they adapt to changing conservation needs for sea otters and other recovering marine mammals.

MANAGEMENT IMPLICATIONS

The results of our study provide estimates of population potential for southern sea otters (Table 3) that can be used for projecting future growth and evaluating population status at regional and sub-regional spatial scales. Our results can facilitate identification of areas within currently unoccupied habitats (Figs. 5B and S4) where potential hot spots of sea otter abundance overlap with economically valuable commercial or recreational fisheries that are likely to be negatively affected by sea otter recovery (e.g., dive fisheries for urchins or abalone). Such information can be used by managers to anticipate areas of conflict, engage relevant stakeholders, and take preemptive steps towards mitigation. Likewise, fine-scale maps of population potential can be used to identify future hot spots of sea otter abundance where resource conflicts are less likely (e.g., the southern edges of the Channel Islands in Santa Barbara Channel; Fig. 5B). Such areas could be the focus of future conservation efforts because they are likely to support both abundant sea otters and diverse and productive sub-tidal communities.

Our model facilitated the first process-based estimate of OSP for this sub-species, one that incorporates the functional form of density dependence and parameter uncertainty. A meaningful value of OSP for recovering marine mammals represents the abundance at which a population is likely to be sustainable and to exert key functional roles within its ecosystem; OSP is thus a key management target under the MMPA. A high priority future task will be to apply the current model to the remainder of the southern sea otter's range in Oregon and Mexico, once suitable habitat data are available.

ACKNOWLEDGMENTS

Any use of trade, product, or firm names is for descriptive purposes only and does not imply endorsement by the United States Government. The findings and conclusions in this article do not necessarily represent the views of the USFWS. We are grateful to all the participants of the annual range-wide sea otter survey and the Southern Sea Otter Stranding Network, principally the U.S. Geological Survey (USGS), California Department of Fish and Wildlife Marine Wildlife Veterinary Care and Research Center, the USFWS, the Bureau of Ocean Energy Management, the Monterey Bay Aquarium, and The Marine Mammal Center. We thank the many staff and volunteers of the above organizations that have assisted in population surveys and the recovery and analysis of stranded otters. We are especially grateful to M. A. Miller, J. A. Ames, F. I. Batac, E. Dodd, C. Young, M. M. Staedler, J. A. Fujii, T. E. Nicholson, and K. A. Mayer. The Navair Ranges Sustainability Office of the United States Navy is acknowledged for access to and logistical support for the sea otter surveys at San Nicolas Island. This research was supported in part by the USGS Ecosystems Mission Area and by the National Science Foundation (NSF) Grant OCE-1538582.

LITERATURE CITED

Banerjee, S., M. M. Wall, and B. P. Carlin. 2003. Frailty modeling for spatially correlated survival data, with application to infant mortality in Minnesota. Biostatistics 4:123–142.

Behrenfeld, M. J., and P. G. Falkowski. 1997. Photosynthetic rates derived from satellite-based chlorophyll concentration. Limnology and Oceanography 42:1–20.

Bell, T., K. Cavanaugh, and D. Siegel. 2017. SBC LTER: Time series of quarterly NetCDF files of kelp biomass in the canopy from Landsat 5, 7 and 8, 1984–2016. https://doi.org/10.6073/pasta/817d2c24ebd78621869e17d94ba0df0c. Accessed 28 Aug 2019.

Bell, T. W., J. G. Allen, K. C. Cavanaugh, and D. A. Siegel. 2020. Three decades of variability in California's giant kelp forests from the Landsat satellites. Remote Sensing of Environment 238:110811.

Besag, J. 1974. Spatial interaction and the statistical analysis of lattice systems. Journal of the Royal Statistical Society: Series B (Methodological) 36:192–225.

Beschta, R. L., and W. J. Ripple. 2009. Large predators and trophic cascades in terrestrial ecosystems of the western United States. Biological Conservation 142:2401–2414.

Bodkin, J. L. 2015. Historic and contemporary status of sea otters in the North Pacific. Pages 43–61 *in* J. L. Bodkin, G. R. Vanblaricom, and S. Larson, editors. Sea otter conservation. Academic Press, Boston, Massachusetts, USA.

Bodkin, J. L., A. M. Burdin, and D. A. Ryazanov. 2000. Age- and sex-specific mortality and population structure in sea otters. Marine Mammal Science 16:201–219.

Bodkin, J. L., G. G. Esslinger, and D. H. Monson. 2004. Foraging depths of sea otters and implications to coastal marine communities. Marine Mammal Science 20:305–321.

Bodkin, J. L., and M. S. Udevitz. 1999. An aerial survey method to estimate sea otter abundance. Pages 13–26 *in* G. W. Garner, S. C. Amstrup, J. L. Laake, B. F. J. Manly, L. L. McDonald, and D. G. Robertson, editors. Marine mammal survey and assessment methods. A. A. Balkema, Leiden, Netherlands.

Breed, G. A., E. A. Golson, and M. T. Tinker. 2017. Predicting animal home-range structure and transitions using a multistate Ornstein-Uhlenbeck biased random walk. Ecology 98:32–47.

Bruckmeier, K., H. Westerberg, and R. Varjopuro. 2013. Baltic seal reconciliation in practice. Pages 15–48 *in* R. Klenke, I. Ring, A. Kranz, N. Jepsen, F. Rauschmayer, and K. Henle, editors. Human-wildlife conflicts in Europe. Springer, Berlin, Germany.

Buckland, S. T., K. B. Newman, L. Thomas, and N. B. Koesters. 2004. State-space models for the dynamics of wild animal populations. Ecological Modelling 171:157–175.

Burt, J. M., M. T. Tinker, D. K. Okamoto, K. W. Demes, K. Holmes, and A. K. Salomon. 2018. Sudden collapse of a mesopredator reveals its complementary role in mediating rocky reef regime shifts. Proceedings of the Royal Society B 285:20180553.

Butler, J., J. Young, I. McMyn, B. Leyshon, I. Graham, I. Walker, J. Baxter, J. Dodd, and C. Warburton. 2015. Evaluating adaptive co-management as conservation conflict resolution: learning from seals and salmon. Journal of Environmental Management 160:212–225.

Buxton, R. T., C. Jones, H. Moller, and D. R. Towns. 2014. Drivers of seabird population recovery on New Zealand islands after predator eradication. Conservation Biology 28:333–344.

Campanyà-Llovet, N., P. V. Snelgrove, and F. C. De Leo. 2018. Food quantity and quality in Barkley Canyon (NE Pacific) and its influence on macro-infaunal community structure. Progress in Oceanography 169:106–119.

Carpenter, B., A. Gelman, M. D. Hoffman, D. Lee, B. Goodrich, M. Betancourt, M. Brubaker, J. Guo, P. Li, and A. Riddell. 2017.

Stan: a probabilistic programming language. Journal of Statistical Software 76:32.
Carr, M. H., and J. E. Caselle. 2018. Partnership for Interdisciplinary Studies of Coastal Oceans (PISCO) Subtidal: Community Surveys: Swath Surveys. PISCO, Corvallis, Oregon, USA. https://doi.org/10.6085/AA/pisco_subtidal.151.2
Carswell, L. P., S. G. Speckman, and V. A. Gill. 2015. Shellfish fishery conflicts and perceptions of sea otters in California and Alaska. Pages 333–368 *in* J. L. Bodkin, G. R. VanBlaricom, and S. Larson, editors. Sea otter conservation. Academic Press, Boston, Massachusetts, USA.
Cavanaugh, K. C., D. A. Siegel, D. C. Reed, and P. E. Dennison. 2011. Environmental controls of giant-kelp biomass in the Santa Barbara Channel, California. Marine Ecology Progress Series 429:1–17.
Chaloupka, M., and G. Balazs. 2007. Using Bayesian state-space modelling to assess the recovery and harvest potential of the Hawaiian green sea turtle stock. Ecological Modelling 205:93–109.
Clapham, P. J., A. Aguilar, and L. T. Hatch. 2008. Determining spatial and temporal scales for management: lessons from whaling. Marine Mammal Science 24:183–201.
Clark, J. S., and O. N. Bjørnstad. 2004. Population time series: process variability, observation errors, missing values, lags, and hidden states. Ecology 85:3140–3150.
Coletti, H. A. 2006. Correlating sea otter density and behavior to habitat attributes in Prince William Sound, Alaska: a model for prediction. University of New Hampshire, Durham, USA.
Davis, R. W., J. L. Bodkin, H. A. Coletti, D. H. Monson, S. E. Larson, L. P. Carswell, and L. M. Nichol. 2019. Future directions in sea otter research and management. Frontiers in Marine Science 5:510.
Day, J. W., Jr, C. A. Hall, W. M. Kemp, and A. Yanez-Arancibia. 1989. Estuarine ecology. John Wiley & Sons, Hoboken, New Jersey, USA.
DeMaster, D. P., C. Marzin, and R. J. Jameson. 1996. Estimating the historical abundance of sea otters in California. Endangered Species Update 13:79–81.
Duggins, D. O. 1980. Kelp beds and sea otters: an experimental approach. Ecology 61:447–453.
Eberhardt, L. L. 1995. Using the Lotka-Leslie model for sea otters. Journal of Wildlife Management 59:222–227.
Estes, J. A. 1979. Exploitation of marine mammals: r-selection of K-strategists? Journal of the Fisheries Board of Canada 36:1009–1017.
Estes, J. A. 1990. Growth and equilibrium in sea otter populations. Journal of Animal Ecology 59:385–402.
Estes, J. A., E. M. Danner, D. F. Doak, B. Konar, A. M. Springer, P. D. Steinberg, M. T. Tinker, and T. M. Williams. 2004. Complex trophic interactions in kelp forest ecosystems. Bulletin of Marine Science 74:621–638.
Estes, J. A., D. F. Doak, J. R. Bodkin, R. J. Jameson, D. Monson, J. Watt, and M. T. Tinker. 1996. Comparative demography of sea otter populations. Endangered Species Update 13:11–13.
Estes, J. A., and D. O. Duggins. 1995. Sea otters and kelp forests in Alaska: generality and variation in a community ecological paradigm. Ecological Monographs 65:75–100.
Estes, J. A., and R. J. Jameson. 1988. A double-survey estimate for sighting probability of sea otters in California. Journal of Wildlife Management 52:70–76.
Estes, J. A., and J. F. Palmisano. 1974. Sea otters: their role in structuring nearshore communities. Science 185:1058–1060.
Evans, M. R., K. J. Norris, and T. G. Benton. 2012. Predictive ecology: systems approaches. 367:322–330.
Gagne, R. B., M. T. Tinker, K. D. Gustafson, K. Ralls, S. Larson, L. M. Tarjan, M. A. Miller, and H. B. Ernest. 2018. Measures of effective population size in sea otters reveal special considerations for wide-ranging species. Evolutionary Applications 11:1779–1790.
Gelfand, A. E., and P. Vounatsou. 2003. Proper multivariate conditional autoregressive models for spatial data analysis. Biostatistics 4:11–15.
Gelman, A. 2005. Comment: fuzzy and Bayesian *p*-values and *u*-values. Statistical Science 20:380–381.
Gelman, A. 2006. Prior distributions for variance parameters in hierarchical models (comment on article by Browne and Draper). Bayesian Analysis 1:515–534.
Gelman, A., Y. Goegebeur, F. Tuerlinckx, and I. Van Mechelen. 2000. Diagnostic checks for discrete data regression models using posterior predictive simulations. Journal of the Royal Statistical Society: Series C (Applied Statistics) 49:247–268.
Gelman, A., A. Jakulin, M. G. Pittau, and Y.-S. Su. 2008. A weakly informative default prior distribution for logistic and other regression models. Annals of Applied Statistics 2:1360–1383.
Gerber, L. R., T. Tinker, D. Doak, and J. Estes. 2004. Mortality sensitivity in life-stage simulation analysis: a case study of southern sea otters. Ecological Applications 14:1554–1565.
Gerrodette, T., and D. P. DeMaster. 1990. Quantitative determination of optimum sustainable population level. Marine Mammal Science 6:1–16.
Ghosh, J. K., M. Delampady, and T. Samanta. 2007. An introduction to Bayesian analysis: theory and methods. Springer Science & Business Media, New York, New York, USA.
Gregr, E. J., L. M. Nichol, J. C. Watson, J. K. B. Ford, and G. M. Ellis. 2008. Estimating carrying capacity for sea otters in British Columbia. Journal of Wildlife Management 72:382–388.
Halley, D., and F. Rosell. 2002. The beaver's reconquest of Eurasia: status, population development and management of a conservation success. Mammal Review 32:153–178.
Hatfield, B. B., M. D. Harris, J. A. Ames, M. T. Tinker, and C. Young. 2017. Summary of stranded southern sea otters, 1985–2016 (ver. 2.0, September 2018): U.S. Geological Survey data release. https://doi.org/10.5066/F71J98P4. Accessed 1 Sep 2019.
Hatfield, B. B., J. L. Yee, M. C. Kenner, J. A. Tomoleoni, and M. T. Tinker. 2018*a*. Annual California sea otter census—2018 spring census summary. U.S. Geological Survey data release. https://doi.org/10.5066/P98012HE. Accessed 1 Sep 2019.
Hatfield, B. B., J. L. Yee, M. C. Kenner, J. A. Tomoleoni, and M. T. Tinker. 2018*b*. California sea otter (*Enhydra lutris nereis*) census results, spring 2018: U.S. Geological Survey Data Series 1097. https://doi.org/10.3133/ds1097. Accessed 1 Sep 2019.
Hechinger, R. F., K. D. Lafferty, J. P. McLaughlin, B. L. Fredensborg, T. C. Huspeni, J. Lorda, P. K. Sandhu, J. C. Shaw, M. E. Torchin, K. L. Whitney, et al. 2011. Food webs including parasites, biomass, body sizes, and life stages for three California/Baja California estuaries. Ecology 92:791–791.
Heide-Jørgensen, M. P., K. Laidre, D. Borchers, F. Samarra, and H. Stern. 2007. Increasing abundance of bowhead whales in West Greenland. Biology Letters 3:577–580.
Henkel, L., M. D. Harris, J. Ames, R. G. Ford, M. Staedler, and M. T. Tinker. 2014. Use of decoys to assess effectiveness of aerial surveys for sea otters. California Department of Fish and Wildlife Office of Spill Prevention and Response Technical Report 14–2, Santa Cruz, USA.
Hobbs, N. T., and D. M. Swift. 1985. Estimates of habitat carrying capacity incorporating explicit nutritional constraints. Journal of Wildlife Management 49:814–822.
Huang, S. L., C. Peng, M. Chen, X. Wang, T. A. Jefferson, Y. Xu, X. Yu, Y. Lao, J. Li, and H. Huang. 2019. Habitat configuration for an obligate shallow-water delphinid: the Indo-Pacific humpback dolphin, *Sousa chinensis*, in the Beibu Gulf (Gulf of Tonkin). Aquatic Conservation: Marine and Freshwater Ecosystems 29:472–485.
Hughes, B. B., R. Eby, E. Van Dyke, M. T. Tinker, C. I. Marks, K. S. Johnson, and K. Wasson. 2013. Recovery of a top predator mediates negative eutrophic effects on seagrass. Proceedings of the National Academy of Sciences of the United States of America 110:15313–15318.
Hughes, B. B., K. Wasson, M. T. Tinker, S. L. Williams, L. P. Carswell, K. E. Boyer, M. W. Beck, R. Eby, R. Scoles, M. Staedler, et al. 2019. Species recovery and recolonization of past habitats: lessons for science and conservation from sea otters in estuaries. PeerJ 7:e8100.
Iijima, H., and M. Ueno. 2016. Spatial heterogeneity in the carrying capacity of sika deer in Japan. Journal of Mammalogy 97:734–743.
Jameson, R. J., K. W. Kenyon, A. M. Johnson, and H. M. Wight. 1982. History and status of translocated sea otter populations in North America. Wildlife Society Bulletin 10:100–107.
Jepsen, N., and T. Olesen. 2013. Cormorants in Denmark: re-enforced management and scientific evidence. Pages 165–183 *in* R. Klenke, I. Ring, A. Kranz, N. Jepsen, F. Rauschmayer, and K. Henle, editors. Human-wildlife conflicts in Europe. Springer, Berlin, Germany.
Johnson, S. Y., G. R. Cochrane, N. E. Golden, P. Dartnell, S. R. Hartwell, S. A. Cochran, and J. T. Watt. 2017. The California Seafloor and Coastal Mapping Program—providing science and geospatial data for California's State Waters. Ocean & Coastal Management 140:88–104.
Kenyon, K. W. 1969. The sea otter in the eastern Pacific Ocean. North American Fauna 68:1–352.

Klenke, R., I. Ring, K. S. Máñez, R. Habighorst, V. Weiss, H. Wittmer, B. Gruber, S. Lampa, and K. Henle. 2013. Otters in Saxony: a story of successful conflict resolution. Pages 107–140 *in* R. Klenke, I. Ring, A. Kranz, N. Jepsen, F. Rauschmayer, and K. Henle, editors. Human-wildlife conflicts in Europe. Springer, Berlin, Germany.

Kvitek, R. G., and J. S. Oliver. 1988. Sea otter foraging habits and effects on prey populations and communities in soft-bottom environments. Pages 22–47 *in* G. R. Vanblaricom and J. A. Estes, editors. The community ecology of sea otters. Springer Verlag, New York, New York, USA.

Lafferty, K. D., and M. T. Tinker. 2014. Sea otters are recolonizing southern California in fits and starts. Ecosphere 5:art50.

Laidre, K. L., R. J. Jameson, and D. P. DeMaster. 2001. An estimation of carrying capacity for sea otters along the California coast. Marine Mammal Science 17:294–309.

Laidre, K. L., R. J. Jameson, E. Gurarie, S. J. Jeffries, and H. Allen. 2009. Spatial habitat use patterns of sea otters in coastal Washington. Journal of Mammalogy 90:906–917.

Laidre, K. L., R. J. Jameson, S. J. Jeffries, R. C. Hobbs, C. E. Bowlby, and G. R. VanBlaricom. 2002. Estimates of carrying capacity for sea otters in Washington state. Wildlife Society Bulletin 30:1172–1181.

Larson, S. D., Z. N. Hoyt, G. L. Eckert, and V. A. Gill. 2013. Impacts of sea otter (*Enhydra lutris*) predation on commercially important sea cucumbers (*Parastichopus californicus*) in southeast Alaska. Canadian Journal of Fisheries and Aquatic Sciences 70:1498–1507.

Liu, Y., R. B. Lund, S. K. Nordone, M. J. Yabsley, and C. S. McMahan. 2017. A Bayesian spatio-temporal model for forecasting the prevalence of antibodies to Ehrlichia species in domestic dogs within the contiguous United States. Parasites & Vectors 10:138.

Lotze, H. K., H. S. Lenihan, B. J. Bourque, R. H. Bradbury, R. G. Cooke, M. C. Kay, S. M. Kidwell, M. X. Kirby, C. H. Peterson, and J. B. Jackson. 2006. Depletion, degradation, and recovery potential of estuaries and coastal seas. Science 312:1806–1809.

Lynn, R. J., and J. J. Simpson. 1987. The California Current System: the seasonal variability of its physical characteristics. Journal of Geophysical Research: Oceans 92:12947–12966.

McDonald, S. L., R. L. Lewison, and A. J. Read. 2016. Evaluating the efficacy of environmental legislation: a case study from the US marine mammal Take Reduction Planning process. Global Ecology and Conservation 5:1–11.

Miller, M. A., M. E. Moriarty, L. Henkel, M. T. Tinker, T. L. Burgess, F. I. Batac, E. Dodd, C. Young, M. D. Harris, D. A. Jessup, et al. 2020. Predators, disease, and environmental change in the nearshore ecosystem: mortality in southern sea otters (*Enhydra lutris nereis*) from 1998–2012. Frontiers in Marine Science 7:582.

Miller, R. B., and R. Meyer. 2000. Bayesian state-space modeling of age-structured data: fitting a model is just the beginning. Canadian Journal of Fisheries and Aquatic Science 57:43–50.

Miller, R. J., K. D. Lafferty, T. Lamy, L. Kui, A. Rassweiler, and D. C. Reed. 2018. Giant kelp, *Macrocystis pyrifera*, increases faunal diversity through physical engineering. Proceedings of the Royal Society B: Biological Sciences 285:20172571.

Monson, D. H., J. A. Estes, J. L. Bodkin, and D. B. Siniff. 2000. Life history plasticity and population regulation in sea otters. Oikos 90:457–468.

Moxley, J. H., T. E. Nicholson, K. S. Van Houtan, and S. J. Jorgensen. 2019. Non-trophic impacts from white sharks complicate population recovery for sea otters. Ecology and Evolution 9:6378–6388.

Nadon, M. O., J. K. Baum, I. D. Williams, J. M. Mcpherson, B. J. Zgliczynski, B. L. Richards, R. E. Schroeder, and R. E. Brainard. 2012. Re-creating missing population baselines for Pacific reef sharks. Conservation Biology 26:493–503.

Nicholson, T. E., K. A. Mayer, M. M. Staedler, J. A. Fujii, M. J. Murray, A. B. Johnson, M. T. Tinker, and K. S. Van Houtan. 2018. Gaps in kelp cover may threaten the recovery of California sea otters. Ecography 41:1751–1762.

Potvin, F., and J. Huot. 1983. Estimating carrying capacity of a white-tailed deer wintering area in Quebec. Journal of Wildlife Management 47:463–475.

R Core Team. 2014. R: a language and environment for statistical computing. R Foundation for Statistical Computing, Vienna, Austria.

Rechsteiner, E. U., J. C. Watson, M. T. Tinker, L. M. Nichol, M. J. Morgan Henderson, C. J. McMillan, M. DeRoos, M. C. Fournier, A. K. Salomon, L. D. Honka, et al. 2019. Sex and occupation time influence niche space of a recovering keystone predator. Ecology and Evolution 9:3321–3334.

Reisewitz, S. E., J. A. Estes, and C. A. Simenstad. 2006. Indirect food web interactions: sea otters and kelp forest fishes in the Aleutian archipelago. Oecologia 146:623–631.

Riedman, M. L., and J. A. Estes. 1990. The sea otter, *Enhydra lutris*: behavior, ecology and natural history. US Fish and Wildlife Service Biological Report 90:1–126.

Ripple, W. J., and R. L. Beschta. 2007. Restoring Yellowstone's aspen with wolves. Biological Conservation 138:514–519.

Ripple, W. J., and R. L. Beschta. 2012. Trophic cascades in Yellowstone: the first 15 years after wolf reintroduction. Biological Conservation 145:205–213.

Salomon, A. K., B. J. W. Kii'iljuus, X. E. White, N. Tanape, and T. M. Happynook. 2015. First Nations perspectives on sea otter conservation in British Columbia and Alaska: insights into coupled human–ocean systems. Pages 301–331 *in* S. Larson, J. L. Bodkin, and G. R. VanBlaricom, editors. Sea otter conservation. Elsevier, New York, New York, USA.

Schiel, D. R., and M. S. Foster. 2015. The biology and ecology of giant kelp forests. University of California Press, Berkley, USA.

Silliman, B. R., B. B. Hughes, L. C. Gaskins, Q. He, M. T. Tinker, A. Read, J. Nifong, and R. Stepp. 2018. Are the ghosts of nature's past haunting ecology today? Current Biology 28:R532–R537.

Stewart, N. L., B. Konar, and M. T. Tinker. 2015. Testing the nutritional-limitation, predator-avoidance, and storm-avoidance hypotheses for restricted sea otter habitat use in the Aleutian Islands, Alaska. Oecologia 177:645–655.

Tarjan, L. M., and M. T. Tinker. 2016. Permissible home range estimation (PHRE) in restricted habitats: a new algorithm and an evaluation for sea otters. PLoS ONE 11:e0150547.

Taylor, B. L., and D. P. Demaster. 1993. Implications of non-linear density dependence. Marine Mammal Science 9:360–371.

Taylor B. L., P. R. Wade, D. P. De Master, and J. Barlow. 2000. Incorporating uncertainty into management models for marine mammals. Conservation Biology 14:1243–1252.

Thometz, N. M., M. M. Staedler, J. A. Tomoleoni, J. L. Bodkin, G. B. Bentall, and M. T. Tinker. 2016. Trade-offs between energy maximization and parental care in a central place forager, the sea otter. Behavioral Ecology 27:1552–1566.

Tinker, M. T. 2015. The use of quantitative models in sea otter conservation. Pages 257–300 *in* J. L. Bodkin, G. R. Vanblaricom, and S. Larson, editors. Sea otter conservation. Academic Press, Boston, Massachusetts, USA.

Tinker, M. T., D. P. Costa, J. A. Estes, and N. Wieringa. 2007. Individual dietary specialization and dive behaviour in the California sea otter: using archival time-depth data to detect alternative foraging strategies. Deep-Sea Research Part II—Topical Studies in Oceanography 54:330–342.

Tinker, M. T., D. F. Doak, and J. A. Estes. 2008. Using demography and movement behavior to predict range expansion of the southern sea otter. Ecological Applications 18:1781–1794.

Tinker, M. T., D. F. Doak, J. A. Estes, B. B. Hatfield, M. M. Staedler, and J. L. Bodkin. 2006. Incorporating diverse data and realistic complexity into demographic estimation procedures for sea otters. Ecological Applications 16:2293–2312.

Tinker, M. T., V. A. Gill, G. G. Esslinger, B. J. L. M. Monk, M. Mangel, D. H. Monson, W. E. Raymond, and M. Kissling. 2019*a*. Trends and carrying capacity of sea otters in Southeast Alaska. Journal of Wildlife Management 83:1073–1089.

Tinker, M. T., and B. B. Hatfield. 2017. California sea otter (*Enhydra lutris nereis*) census results, spring 2017: U.S. Geological Survey Data Series 1067. https://doi.org/10.3133/ds1067. Accessed 1 Sep 2019.

Tinker, M. T., B. B. Hatfield, M. D. Harris, and J. A. Ames. 2016. Dramatic increase in sea otter mortality from white sharks in California. Marine Mammal Science 32:309–326.

Tinker, M. T., J. Tomoleoni, N. LaRoche, L. Bowen, A. K. Miles, M. Murray, M. Staedler, and Z. Randell. 2017. Southern sea otter range expansion and habitat use in the Santa Barbara Channel, California. OCS Study BOEM 2017-002. U.S. Geological Survey Open File Report No. 2017-1001, Reston, Virginia, USA.

Tinker, M. T., J. A. Tomoleoni, B. P. Weitzman, M. Staedler, D. Jessup, M. J. Murray, M. Miller, T. Burgess, L. Bowen, A. K. Miles, et al. 2019*b*. Southern sea otter (*Enhydra lutris nereis*) population biology at Big Sur and

Monterey, California—investigating the consequences of resource abundance and anthropogenic stressors for sea otter recovery. U.S. Geological Survey Open-File Report No. 2019-1022, Reston, Virginia, USA.
Udevitz, M. S., J. L. Bodkin, and D. P. Costa. 1995. Detection of sea otters in boat-based surveys of Prince William Sound, Alaska. Marine Mammal Science 11:59–71.
U.S. Fish and Wildlife Service [USFWS]. 2003. Final revised recovery plan for the southern sea otter (*Enhydra lutris nereis*). U.S. Fish and Wildlife Service, Washington, D.C., USA.
Vehtari, A., A. Gelman, and J. Gabry. 2017. Practical Bayesian model evaluation using leave-one-out cross-validation and WAIC. Statistics and Computing 27:1413–1432.
Wang, G. 2007. On the latent state estimation of nonlinear population dynamics using Bayesian and non-Bayesian state-space models. Ecological Modelling 200:521–528.
Wang, G. 2009. Signal extraction from long-term ecological data using Bayesian and non-Bayesian state-space models. Ecological Informatics 4:69–75.
Wheeler, S. G., T. W. Anderson, T. W. Bell, S. G. Morgan, and J. A. Hobbs. 2017. Regional productivity predicts individual growth and recruitment of rockfishes in a northern California upwelling system. Limnology and Oceanography 62:754–767.

Associate Editor: James Sheppard.

SUPPORTING INFORMATION

Additional supporting information may be found in the online version of this article at the publisher's website.